MICROSTRIP PATCH BALUN BANDPASS FILTER

NG CHI HWA

A project report submitted in partial fulfilment of the
requirements for the award of the degree of
Bachelor (Hons.) of Electrical and Electronics Engineering

Faculty of Engineering and Science
Universiti Tunku Abdul Rahman

May 2011

DECLARATION

I hereby declare that this project report is based on my original work except for citations and quotations which have been duly acknowledged. I also declare that it has not been previously and concurrently submitted for any other degree or award at UTAR or other institutions.

Signature : _____

Name : NG CHI HWA

ID No. : 07UEB04393

Date : 15th April 2011

APPROVAL FOR SUBMISSION

I certify that this project report entitled **"MIRCROSTRIP PATCH BALUN BANDPASS FILTER"** was prepared by **NG CHI HWA** has met the required standard for submission in partial fulfilment of the requirements for the award of Bachelor of Electrical and Electronics Engineering (Hons.) at Universiti Tunku Abdul Rahman.

Approved by,

Signature : _____

Supervisor : Dr. Lim Eng Hock

Date : _____15th April 2011_____

Specially dedicated to
my beloved parents, coursemates and friends.

ACKNOWLEDGEMENTS

I would like to thank everyone who had contributed to the successful completion of this project. I would like to express my gratitude to my research supervisor, Dr. Lim Eng Hock for his invaluable advice, guidance and enormous patience throughout the development of the research.

In addition, I would also like to express my utmost gratitude to my loving parents and friends who had helped and given me continuous supports throughout this project.

MICROSTRIP PATCH BALUN BANDPASS FILTER

ABSTRACT

Filtering is a very important process in our daily life. When it comes to communication, filter is an essential component that is incorporated into the communication device. Filter is used to eliminate unwanted frequencies or to select desired range of frequencies. A new compact microstrip patch balun bandpass filter has been proposed in this project and fabricated on RT/Duroid 6006 substrate. The novelty of this design is that it divides the microwave signal equally into two with 180^0 out of phase. The project can be separated into three major stages which are simulation, fabrication and experimental stage. A series of simulations based on High Frequency Structure Simulator (HFSS) will be run to simulate the filter design with different configurations and the results are analysed. Frequency response of the fabricated filter is measured by using Vector Network Analyzer (VNA) in laboratory. Experiments have been conducted, with good agreement observed between the simulated and measured results. The insertion loss, return loss and characteristic of the each parameter is been studied. A thorough studies and further discussions have been done on the proposed filter and recommendations have been proposed.

TABLE OF CONTENTS

LIST OF TABLES

LIST OF FIGURES

LIST OF SYMBOLS / ABBREVIATIONS

λ	wavelength, m
f	frequency, Hz
c	speed of light, m/s
ε_r	dielectric constant
ε_{eff}	effective dielectric constant
H	thickness of substrate, mm
W	width of striplines, mm
Z_o	characteristic impedance, Ω
Z_{in}	input impedance, Ω
S_{11}	reflection loss, dB
S_{21}	insertion loss, dB
VNA	Vector Network Analyzer
HFSS	High Frequency Structure Simulator
LTCC	low-temperature co-fired ceramics
HTS	High Temperature Superconductor
MMIC	Monolithic Microwave Integrated Circuits
MEMS	Microelectromechanic System
RF	Radio Frequency
CAD	Computer Aided Design
PCB	Printed Circuit Board
CST	Computer Simulation Technology
GSM	Global System for Mobile Communication

CHAPTER 1

INTRODUCTION

1.1 Background

Bandpass filter is an electronic device that passes frequencies within a certain range and rejects frequencies outside that range. Bandpass filters can be classified into 2 categories: active and passive filters. An active bandpass filter requires an external power source, and it employs active components such as transistors and integrated circuits. It uses no external power source and consists only of passive components such as capacitors and inductors. Such configurations are referred to as passive filters.

Bandpass filters are used primarily in wireless transmitters and receivers. In transmitters, the main function of such filters is to limit the bandwidth of output signals so that power utilization can be more efficient. For a receiver, bandpass filters remove noise from the received signal and allow only signals within certain ranges of frequencies to pass through. Therefore, the use of bandpass filters can improve the signal-to-noise ratio significantly.

In applications for both the transmitter and receiver, the optimized filters must be operating in one or more than one passbands so that it can maximize the number of channels transferring in a system, while minimizing the interference or competition among signals.

A microstrip filter is different from those ordinary filters operating at low frequencies, where capacitors and inductors are broadly used. Microstrip filter is

usually fabricated on a substrate and it does not use any electronic components. The advantages of microstrip filter are small size, low cost, easy to fabricate, high performance, and multi-frequency nature. According to IEEE Xplore, there have been more than 600 publications related to microstrip filters in recent 10 years.

1.2 Research Aims and Objectives

The objective of this project is to design a microstrip dual-mode bandpass filter that function as a balun at the same time using Ansoft High Frequency Structure Simulator (HFSS). HFSS is a 3D Full-wave Electromagnetic Field Simulation software. The fundamental knowledge in microstrip filter is vital in order to design a filter with a unique configuration. Therefore, research had been done base on the microstrip filter journals and articles that are available in IEEE Xplore database under the UTAR OPAC system. After acquiring information and ideas from the literature survey, a new design was implemented on designing the filter.

The aim of this project is to design a microstrip dual-mode balun filter with good performance, ease of fabrication and simplicity. The filter is designed so that it will have a dual-mode characteristic and the resonant frequency range must be in between 1 to 6 GHz. There is no limitation on the size and shape of the patch and the type of substrate used. However, size of the filter is vital in communication system as devices are getting smaller so miniature size is also one of the aim of the design. In addition, the filter design consists of 3 ports with 1 input and 2 outputs. The aim is to design a filter where the input of the microwave signal is equally divided into two so that it is also a good balun filter.

On completion of this project, students will attain knowledge on how to carry out research, working principles of microstrip patch filter and criteria on designing a filter with good performance. Besides that, they are able to design any microwave devices such as antenna or filter by using High Frequency Structure Simulator (HFSS). Students are exposed to fabrication process, experimental process and high frequency measurement equipment in this project. Experiments are done by using

Vector Network Analyzer to measure the experimental results to verify with the simulated results. Analysis of the results can be used to further improve the filter design.

1.3 Project Motivation

The motivation of the project is to design a microstrip patch balun bandpass filter that has good performance and publishable in an international journal. After some literature surveys, most of the rectangular patch filters are publishable and easier to design compare with other patch shapes. Some of the filters that had been proposed are larger in size where size of the filter is taken into consideration in small devices. Hence, the motivation of the project is to use a rectangular patch to design a filter and a balun at the same time. Moreover, the motivation is to design a compact size microstrip patch filter that able to produce a comparable result to the journal that had been published. In addition, the novelty of the filter is it is able to divide the microwave signal equally into two with 180^0 out of phase.

CHAPTER 2

LITERATURE REVIEW

2.1 About Microstrip Filter

Microwave filters are playing important roles in various fields and industries such as Radio Frequency (RF), wireless communication and microwave applications. The development of microstrip filters has been in great demand due to the rapid growth of wireless communication systems in this decade. The main purpose of filter is to pass and reject desired band of frequencies. With the advancement of microwave field and its achievement, it has imposed rigorous standards of performance requirement on RF and microwave filters. Moreover, with recent development in wireless communication, microstrip filters have been widely used in various applications of satellite, microwave circuits, radar systems and mobile communication systems due to its compact size and low loss characteristic. The features such as small size, low mass, low loss, ease of fabrication, high performance and multi-frequencies properties of microstrip filter are highly demand by the market. In addition, the recent advance in novel materials and fabrications technologies such as low-temperature co-fired ceramics (LTCC), high-temperature superconductor (HTS), monolithic microwave integrated circuits (MMIC), microelectromechanic system (MEMS) and micromachining technology had increased the development of the new microstrip filter to a higher level.

The invention of computer-aided design (CAD) tool such as Computer Simulation Technology (CST) and High Frequency Structure Simulator (HFSS) makes the work of designing RF and microwave design simple. Hence, designing

microstrip filter is easier and it has reduced the cost of research on microstrip filter. The reasons are that designers are able to obtain the results and observation can be done on the simulated results without any fabrication. The development in microwave designing tools and increase of computer processing power had contributed to the growth of microwave research area. A powerful CAD tool is able to produce simulation results that are comparable to experimental results which give a high degree of accuracy. Ansoft High Frequency Structure Simulator (HFSS) has been used in this project as CAD tools for the microstrip filter design.

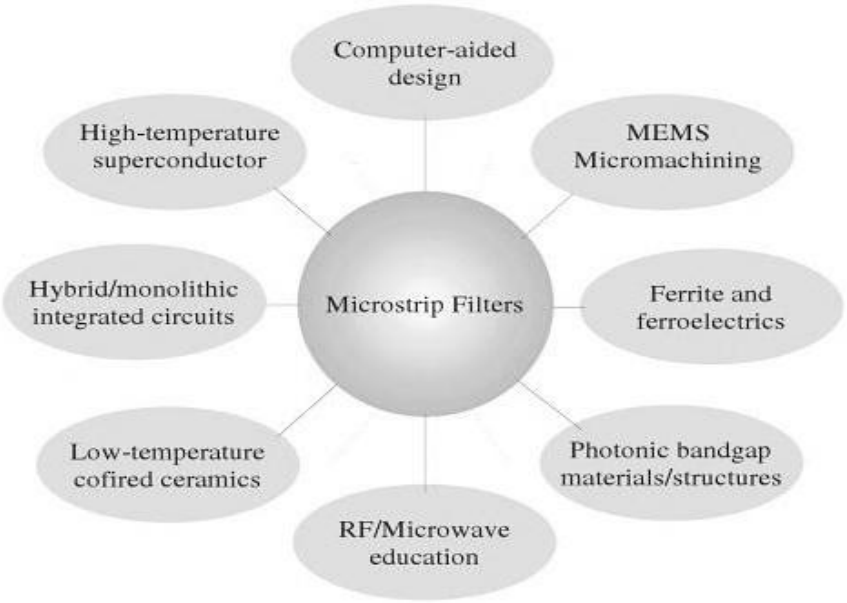

Figure 2.1: Microstrip filters linkage.

There are various kinds of microstrip filters that had been published in the past. Different designs of filter have different types of characteristics and properties. Filter can be designed in variety patterns for different requirements and purposes. Some of the common microstrip filter designs are microstrip lines filter, rectangular patch filter, circular patch filter, rectangular ring filter and circular ring filter. The figures below show few examples of filter designs that had been published in the past.

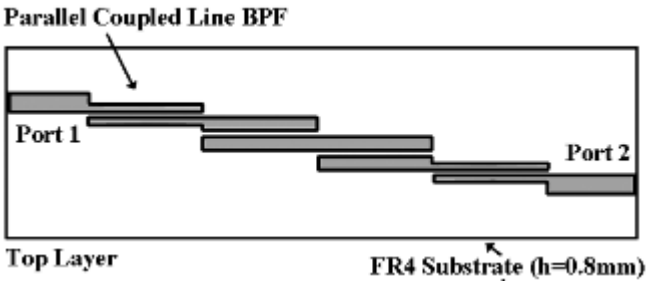

Figure 2.2: Design of parallel couple microstrip lines bandpass filter

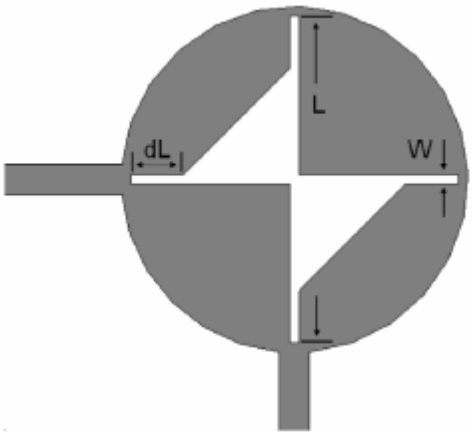

Figure 2.3: Design of microstrip-fed dual-mode filter with crossed slot and two triangular perturbation elements at the center

Figure 2.4: Conventional design of triangular resonator dual-mode filter

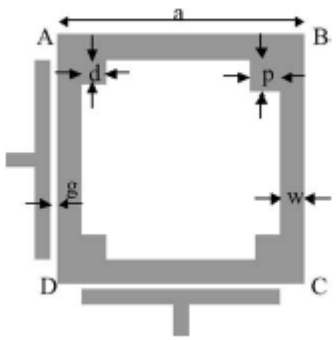

Figure 2.5: Dual-mode microstrip loop resonator design

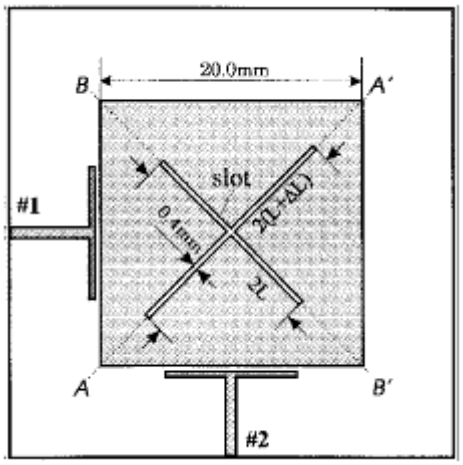

Figure 2.6: Crossed slot microstrip rectangular patch bandpass filter design

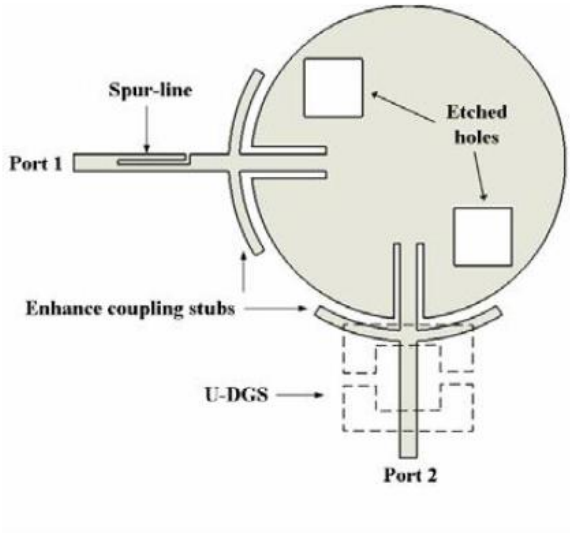

Figure 2.7: Circular patch bandpass filter with multi-order harmonic suppressed I/O lines design

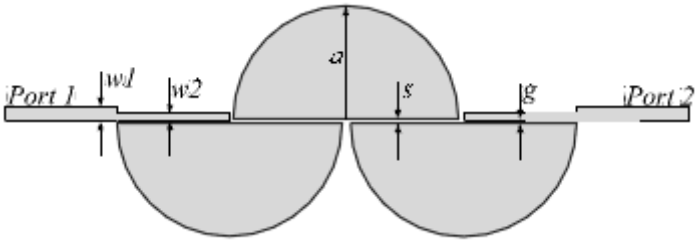

Figure 2.8: Three-pole microstrip semi-circular bandpass filter design

2.1.1 Microstrip Lines

Microstrip is a planar transmission lines which similar to the stripline and coplanar waveguide. It consists of a conductive strip and a ground plane separated by a layer of dielectric in between which also known as the substrate. Microstrip was first developed by ITT laboratories for defeating stripline and it had been published by Grieg and Engelmann in December 1952. The early microstrip work uses fat substrates to allow non-TEM waves to propagate which makes results unpredictable. Microstrip lines is one of the most popular types of planar transmission lines, primarily because it can be fabricated by photolithographic process and is easily integrated with other passive and active microwave devices.

Microstrip can be fabricated using printed circuit board (PCB) technology and it is used to convey microwave-frequency signals. Figure 2.9 shows an example of a simple cross-section of microstrip geometry as described earlier. It can be seen that section A is a conducting strip separated from a ground plane (section D) by a dielectric layer known as the substrate (section C) while section B is air.

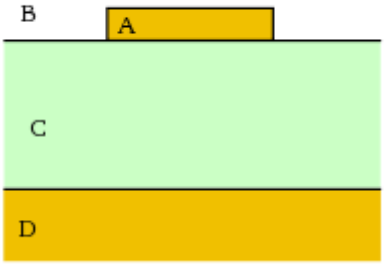

Figure 2.9: Cross-section of microstrip geometry.

Microwave components such as antennas, couplers, filters, and power dividers can be formed from microstrip. The whole device is just a pattern of metallization on the substrate. The microstrip is gaining popularity due to the cost which is much less expensive, far lighter and more compact than traditional waveguide technology. However, the disadvantages of microstrip are the generally lower power handling capacity and higher losses compared with waveguide. Moreover, microstrip is not enclosed, and is therefore susceptible to cross-talk and unintentional radiation.

In this project, microstrip has been chosen for the filter design because the dielectric losses is reasonable for microwave device and has higher dielectric constant compare to FR-4 substrate. In addition, the workability and effectiveness of microstrip is proven by thousands of experiments that had been carried out in the past compare to other substrates. The shielding problem can be easily solved by placing the filter inside a box. The cross-talk and unintentional radiation is not an issue in filter design as it is more prone towards antenna design. Moreover there are few decades of maturity in microstrip and references are easy available in IEEE Xplore database.

2.1.1.1 Dielectric Constant

The dielectric constant of a material is the ratio of its permittivity to the permittivity of vacuum. The dielectric constant is also known as the relative

permittivity of the material. Hence, it is a measure of the extent to which it concentrates electrostatic lines of flux. Different substrates are made from different materials which have different dielectric constants. Microstrip can be fabricated on different substrates based on the requirement of the design. Some designs do not require high dielectric constant and therefore FR-4 substrate which has dielectric constant of 4.4 can be use. FR-4 substrate is much cheaper as compared to RT/Duroid 6006 which has dielectric constant of 6.15. Dielectric constant is frequency dependent. For instance, the dielectric of FR-4 is 4.35 at 500MHz and 4.34 at 1GHz. There is a 0.01 difference in the dielectric constant in 500MHz variation, which is around 0.23% variation per 500MHz.

In this project, RT/Duroid 6006 has been chosen as the substrate for the microstrip filter design because it require higher dielectric constant which having lower losses. In addition, the filter design in this project is in the range of high frequency where FR-4 will not be suitable to use as a substrate. Although RT/Duroid 6006 is more expensive, the cost will not put on priority due to the filter design requirement. The substrate is expensive because it is relatively thin and high in dielectric constant. RT/Duroid 6006 substrate is not available in the Malaysia and has to order from Rogers Corporation in United State. The substrate came with a dimension of 25.4cm x 25.4cm.

2.1.1.2 Effective Dielectric Constant

Effective dielectric constant can be interpreted as the dielectric constant of a homogeneous medium that replaces the air and the dielectric regions of the microstrip. In general, the dielectric constant of a substrate will be greater than air. Hence the electromagnetic wave is travelling in an inhomogeneous medium and propagation velocity is affected by the dielectric constant. The propagation velocity falls between the speed of radio waves in the substrate and the speed of radio waves in air. Normally, the effective dielectric constant is slightly less than the substrate dielectric constant because part of the fields from the microstrip conductor exists in the air.

According to Bahl and Trivedi, the effective dielectric constant can be calculated by using the formula below where *W* represents the width of the microstripline, *H* is the height of the substrate and Ɛr represents dielectric constant of the substrate. There are separate solutions for cases where *W/H* is less than 1 and when *W/H* is greater than or equal to 1. The formula used is just a reasonable approximation for the effective dielectric constant because it ignored microstrip lines thickness and frequency dispersion. However their effects are usually small and reasonably acceptable.

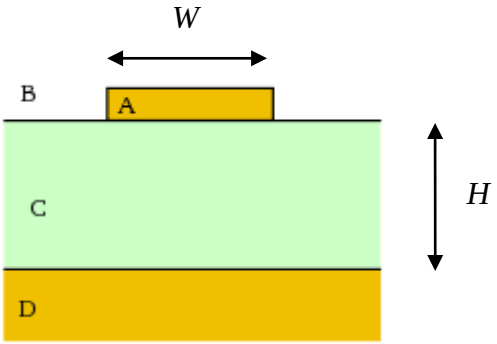

Figure 2.10 : Substrate

$$when \left(\frac{W}{H}\right) < 1$$

$$\varepsilon_e = \frac{\varepsilon_r + 1}{2} + \frac{\varepsilon_r - 1}{2}\left[\left(1 + 12\left(\frac{H}{W}\right)\right)^{-1/2} + 0.04\left(1 - \left(\frac{W}{H}\right)\right)^2\right]$$

$$when \left(\frac{W}{H}\right) \geq 1$$

$$\varepsilon_e = \frac{\varepsilon_r + 1}{2} + \frac{\varepsilon_r - 1}{2}\left(1 + 12\left(\frac{H}{W}\right)\right)^{-1/2}$$

The inhomogeneous medium will cause the line to not support a true TEM wave at non-zero frequencies, and both E field and H field will have longitudinal components. However, the longitudinal components are small and the dominant mode is referred to as quasi-TEM. Meanwhile, the microstrip lines are dispersive in inhomogeneous medium. The effective dielectric constant will gradually increase towards the substrate with the increasing frequency so that the phase velocity will slowly decrease.

In this project, High Frequency Structure Simulator, HFSS has taken effective dielectric constant into the account during simulation process where the air box structure came into the part. All the necessary calculation had been done automatically by the simulation software.

2.1.1.3 Characteristic Impedance

The characteristic impedance or surge impedance of a uniform transmission line, usually written as Z_0, is the ratio of the amplitudes of a single pair of voltage and current waves propagating along the line in the absence of reflections. The characteristic impedance, Z_o plays an important role in microstrip lines design which will affects the reflection loss, S_{11}. The reflection loss is related to characteristic impedance by formula, $S_{11} = \frac{Z_{in} - Z_o}{Z_{in} + Z_o}$. From the formula, in order to minimize the reflection loss at the input port, the characteristic impedance of microstrip must be equal to the input impedance. In this project, the input impedance is the Vector Network Analyzer (VNA) connector input impedance. Most of the input ports are designed at to be 50ohm. Hence, reflection loss can be reduced to the minimum by designing the microstrip lines to be 50ohm. This is called impedance matching.

In general, non-TEM structures such as microstrip lines have characteristic impedance which is not unique. It has been a fact that the cause of this uncertainty is due to the longitudinal field components of non-TEM modes. Due to this component, the current and voltage are not uniquely defined in terms of the usual TEM path integrals of the fields. According to Bahl and Trivedi, the characteristic impedance of microstrip lines can be calculated by using the formula below.

$$when \left(\frac{W}{H}\right) < 1$$

$$Z_0 = \frac{60}{\sqrt{\varepsilon_{eff}}} \ln\left(8\frac{H}{W} + 0.25\frac{W}{H}\right) \ (ohms)$$

$$when \left(\frac{W}{H}\right) \geq 1$$

$$Z_0 = \frac{120\,\pi}{\sqrt{\varepsilon_{eff}} \times \left[\frac{W}{H} + 1.393 + \frac{2}{3}\ln\left(\frac{W}{H} + 1.444\right)\right]} \ (ohms)$$

Similar to the effective dielectric constant, the characteristic impedance is also a function of the ratio of the height to the width *W/H* of microstrip lines. The effective dielectric constant value is needed to obtain the microstrip characteristic impedance.

From the very beginning in the designing stage, the microstrip lines must be designed in such a way that the characteristic impedance must be 50 ohm. This can be done by using the above formula or software that is available from the web. If the formula is used to calculate the characteristic impedance, the parameters that are needed are $\mathcal{E}_{eff}$, width(*W*), height(*H*) and the ratio of *W/H* to determine which formula to be use. This method is complicated and it is time consuming. Hence another method is chosen where the software is used to calculate the width of the microstrip lines. In order to get the value of the width of the microstrip lines, the desire characteristic impedance, height of the substrate, the thickness of the microstrip lines and dielectric constant of the substrate is enter and within a second the width of the microstrip lines has been calculated. TX Line 2003 software is used for the calculation.

2.1.2 Microstrip Resonators

Microstrip resonators can be found in various shapes and designs depending on the requirement of the filters. A research on the microstrip resonators has been done by reading some related journals that are available from IEEE Xplore database before the designing stage. The performance of a microstrip filter is very dependent on the resonator design. A small change in resonator design will give a tremendous

effect on the results. The author has chosen a few types of resonators that will be discussed in more detail in next sub-chapter. The types of resonators that will be discussed are cross-slotted patch resonator, circular patch resonator and triangular loop resonator.

2.1.2.1 Cross Slotted Patch Resonator

In this section, a journal with the title "New Planar Dual-Mode Filter Using Cross-Slotted Patch Resonator for Simultaneous Size and Loss Reduction" by Lei Zhu, Pierre-Marie Wecowski, and Ke Wu published in IEEE Transactions on Microwave Theory and Techniques, Vol. 47, No. 5, May 1999 will be review. A new concept had been used in this journal where a pair of unequal cross-slots are use to form on a square patch resonator so that its radiation loss and structure size can be significantly reduced simultaneously.

Besides that, the dual-mode concept is stemmed from a physical coupling of two degenerate modes in a geometrically symmetrical resonator such as ring or patch resonators. Perturbation element is usually added at a certain position of a resonator in order to slightly degrade its geometrical symmetry. Moreover, the coupling behavior of a dual-mode patch resonator is studied in connection with the two unequal slots length, indicating some attractive filtering characteristic of proposed filter.

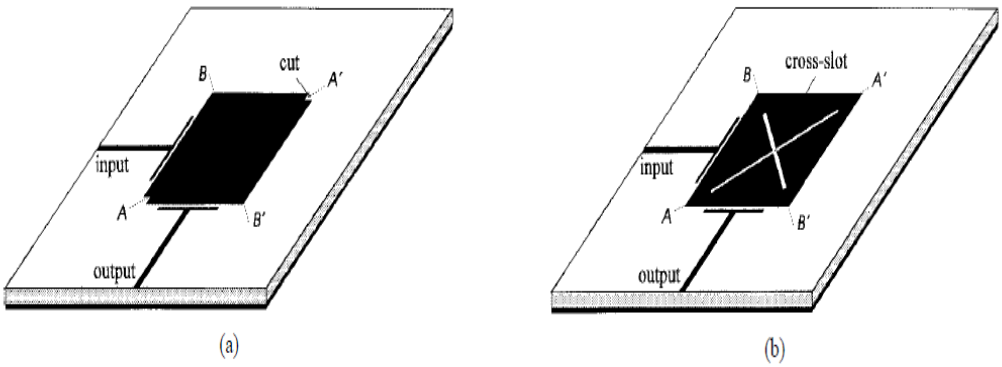

Figure 2.11: Geometry of two classes dual-mode planar filter (a) Conventional type (b) Novel type

A brief physical description is done based on Figure 2.11. In Figure 2.11 (a) shows a dual-mode bandpass filter on the basis of a conventional microstrip patch resonator incorporating the perturbation element, which is simply a pair of corner cuts at its diagonal plane A-A'. Figure 2.11 (b) shows a proposed dual-mode filter in this journal at which the open patch resonator is etched by a pair of electrically narrow crossed slots that are oriented along its two diagonal plane A-A' and B-B' respectively.

Based on the two filter designs, it is well understood that the coupling strength of the two modes depends on the physical geometry of the perturbation element at it is usually designated to be relatively weak in the case of designing a dual-mode filter with low insertion lost and narrow-band operation. Strong capacitive coupling strength can be achieved by stretching out the open ends of the two lines along the periphery of the patch resonator. The loss of this type of dual-mode filter which is the limiting factor in designing high-Q filter is basically caused by conductor loss from the line with narrow strip width and radiation loss from the open patch resonator. This can be overcome by choosing an electrically thin dielectric substrate. However this will contribute to increase of conductor loss.

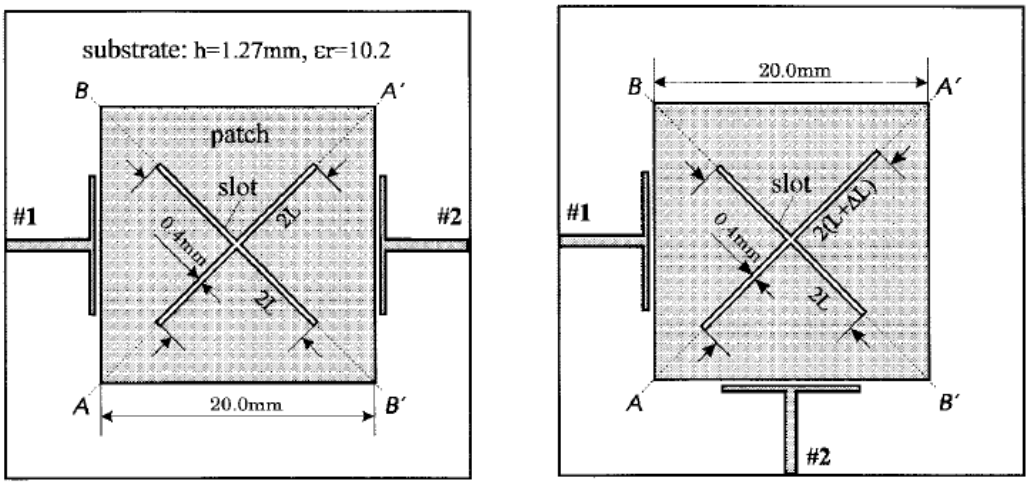

(a) (b)

Figure 2.12: (a) Top view of a single-mode patch resonator etched with a pair of symmetrical crossed slots, (b) Geometrical view of planar dual-mode filter etched with a pair of asymmetrical crossed slots with build-in control element of mode coupling or perturbation

The features of a single mode resonator circuit are applied to the design of a low loss dual-mode filter by rearranging the orientation of the two externally connected lines and also by adequately differentiating the two slots length to produce the coupling between the two degenerate modes. The perturbation element introduced is similar to the corner cut which is responsible for the coupling between the degenerate modes in the patch resonator.

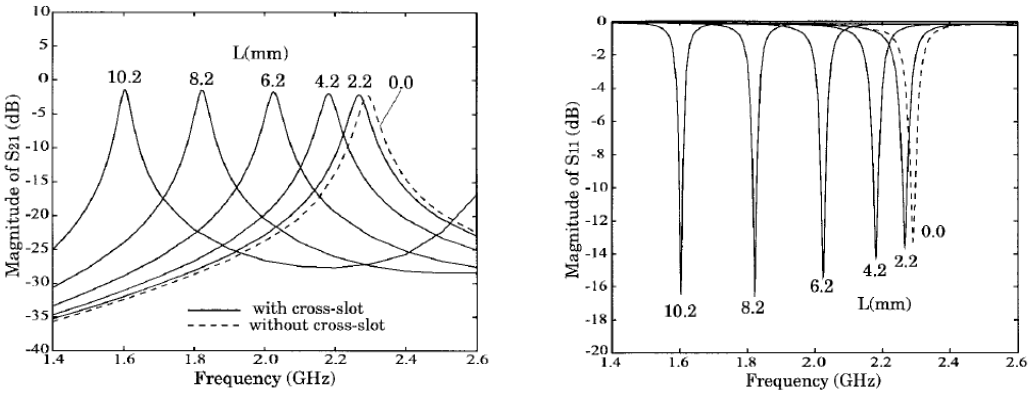

(a) (b)

Figure 2.13: Simulated frequency response of a single mode resonator for differential length of symmetrical crossed slots, (a) Insertion loss (b) Return loss

From the Figure 2.13, it can be observed that the curves of fundamental resonant frequency is shifted to the left as the slot length increases while the peak point of S_{21} increased slightly and the frequency bandwidth becomes gradually narrow. The effect of the crossed slots is very significant in the design. The resonant frequency is greatly reduced from 2.29 to 1.6 GHz.

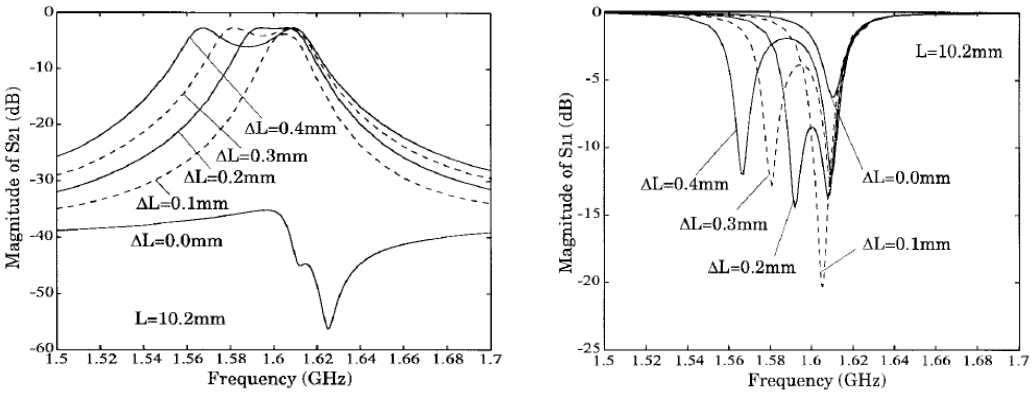

(a) (b)

Figure 2.14: Simulated frequency response of dual-mode filtering behaviour in connection with the difference of the two unequal crossed slots length ΔL, (a) Insertion loss (b) Return loss

From the above figure, it can be seen that there is no coupling between the two modes as ΔL = 0mm. It is found in this case that S_{21} is lower than -35dB over the frequency range of 1.5-1.7 GHz, showing excellent isolation between the two modes. Nevertheless, the parasitic mode to mode coupling still appears even though it is very weak due to the asymmetrical arrangement of the two external lines. S_{21} moves rapidly upward to -4.5 dB and S_{11} goes down next to -20dB at the center frequency as ΔL is increased to 0.1mm.

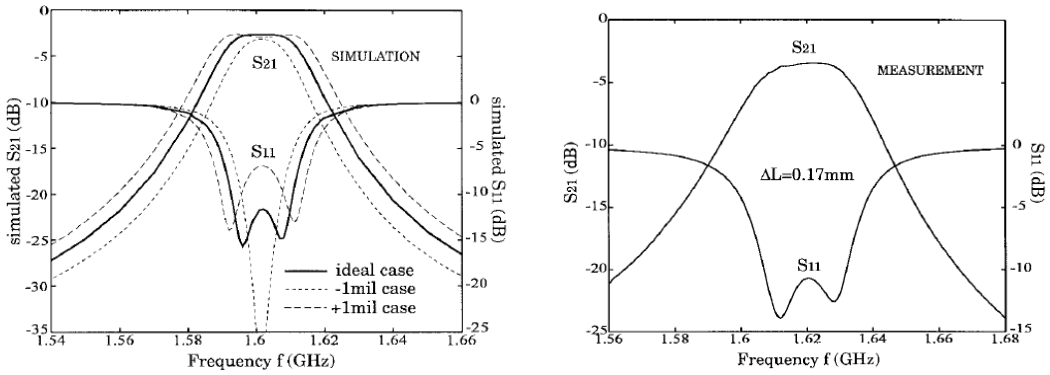

(a) (b)

Figure 2.15: Comparison between frequency response of (a) Simulated results and (b) Measured results.

The simplicity of the design in Zhu Lei paper has provides very useful information towards this project to the author. The features of the filter in this paper such as compact size and low radiation loss of rectangular patch resonator can be used in this project. This paper serves as a general guideline in designing the filter.

2.1.2.2 Circular Patch Resonator

The title "Characteristics of a Microstrip Semi-Circular Patch Resonator Filter" by Kittisak Phaebua and Chuwong Phongcharoenpanich will be discussed. Coupling coefficient of inter-coupled resonator and external quality factors of the input and output of the resonator determined the design method. Semi-circular patch resonators are used instead of the microstrip circular patch resonator to improve the filter characteristics by using the coupling structure.

For a microstrip filter design, it is important to select a suitable type of resonator. There are several types of resonators such as the half wave length transmission line resonator, circular patch resonator, triangle patch resonator, open loop resonator and hairpin resonator. The circular patch resonator has been considered for many applications due to higher Q-factor compare to other types of resonators. In addition, the selectivity of filter depends on the amount of resonators for high performance filter. However, the circular patch resonator yields weakly coupling coefficient affected to small spacing between resonators. This caused the structure to be more complicated and requires high technologies for filter fabrication.

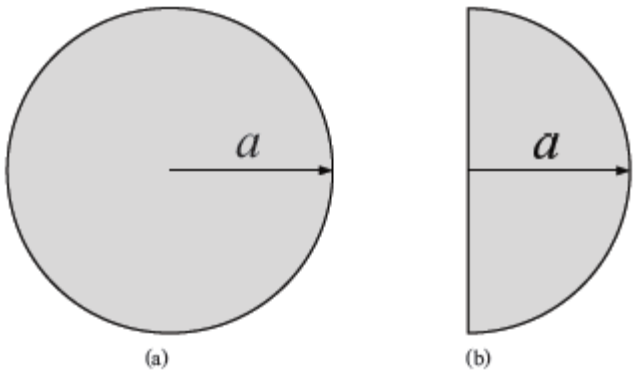

Figure 2.16: (a) Microstrip Circular Patch Resonator ,
(b) Microstrip Semi-Circular Patch Resonator

The resonant frequency must be known before designing any microstrip filter. In order to design a circular patch resonator, the dominant mode (TM_{110}) is considered. Hence the resonant frequency can be calculated using the formula, $(f_r)_{110} = \frac{1.8412\,c}{2\pi a\sqrt{\varepsilon_r}}$ where c is the speed of light and a represent the radius of the

circular patch. The substrate used in designing this filter is Roger RT 3003 with dielectric constant of 3, and thickness of the substrate is 0.764mm. Figure 2.17 shows a graph of resonant frequency versus the radius of the circular patch. In the journal, the author designed a 2GHz resonant frequency resonator with 25 mm of radius.

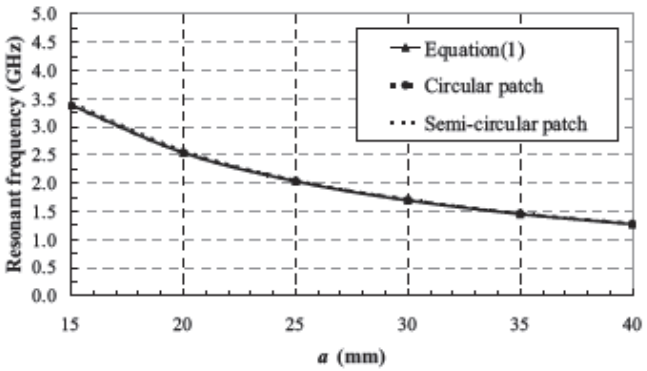

Figure 2.17: Resonant Frequency versus Circular Patch Radius

Improvement has been done by modifying the ordinary semi-circular patch resonators into a novel three-pole bandpass filter as shown in Figure 2.18. The coupling effect of the microstrip resonator is studied in the journal. In Figure 2.19, it is shown that the coupling coefficient is decreases exponentially when the gap between resonators increases. Base on calculation, the coupling coefficient is 0.021 and a gap of 1mm has been used between the semi-circular resonators.

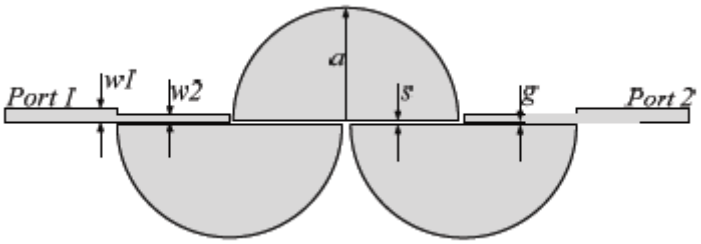

Figure 2.18: Three-pole Microstrip Semi-circular Bandpass Filter

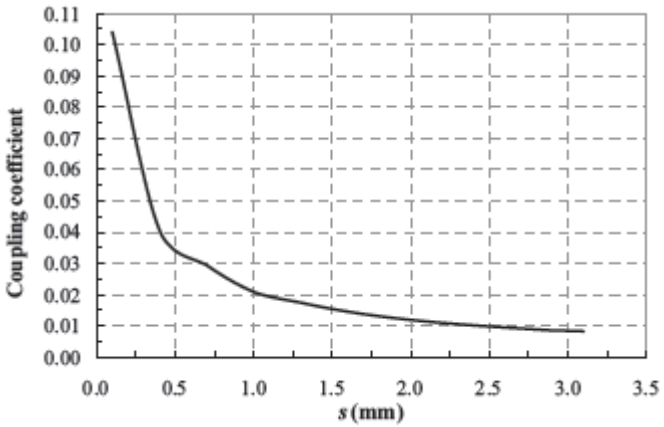

Figure 2.19: Coupling Coefficient of Microstrip Semi-circular Patch Resonator

After research has been done on the journal, different methods are used to design a circular patch resonator compare to rectangular ring resonator. Firstly, the radius of circular patch resonator will determine the resonant frequency of the resonator. However, it is also dependent on which dominant mode is considered. In this journal, TM_{110} has been considered during the circular patch resonator design. Besides, the coupling coefficient is affected the gap between the circular resonators. Based on the formula provided in the journal, the designer is able to calculate the coupling coefficient and hence determine the gap between resonators.

In conclusion, circular resonators are harder to design compare to rectangular patch resonator due to the shape. This has narrowed down research direction to rectangular patch as it is less complicated.

2.1.2.3 Triangular Patch Resonator

Microstrip triangular resonator has important applications in microwave circuits especially the equilateral triangular resonator. Triangular resonator can be designed in single triangular patch or fractal triangular patch. In this paper entitle "Novel Microstrip Triangular Resonator Bandpass Filter with Transmission Zeros and Wide Bands Using Fractal Shaped Defection" by J.K Xiao, Q.X Chu and S.Zhang will be discussed. Fractal means broken or fractured which is derived from

Latin word “fractus”. Advantages of a fractal triangular patch resonator are the miniaturization and wide band or multi-band operation. For a patch resonator filter, fractal defection can act as filter perturbation which may suppress the undesired harmonics and implement wide stopband.

A novel fractal bandpass filter using equilateral triangular resonator is presented by Xiao and Chu to implement high performance of multi transmission zeros, wide passband and stopband and low passband insertion loss as well as miniaturization. The configuration of the microstrip equilateral triangular resonator with fractal shaped defection is shown in Figure 2.20 where ‘a’ is triangle side length, ‘b’ is the length of triangle defection hemline and ‘h’ is defection height.

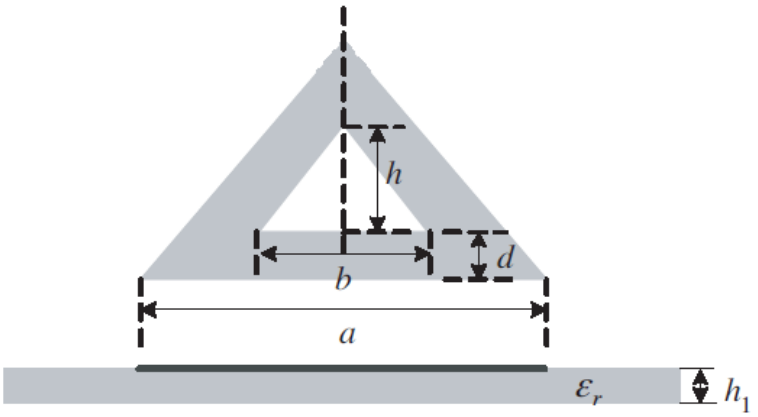

Figure 2.20: Microstrip equilateral triangular resonator with fractal shaped defection

The proposed bandpass filter having better performance of wider passband, multi transmission zeros, wider stopband, simple configuration and miniaturization which due to single patch operation. In addition, designing and fabrication will be easier due to the simple structure. Resonant characteristics of equilateral triangular resonator with and without fractal shaped defection can be calculated using the formula. EM simulation and magnetic field pattern of resonator with fractal shaped defection is shown in Figure 2.21 to Figure 2.24. Figure 2.21, Figure 2.22 and Figure 2.23 show the characteristics of microstrip equilateral triangular resonator with and without fractal shaped defection. Figure 2.23 shows the relationship of fractal defection height and resonant frequencies for different resonant modes. From the figure it can be observed that the dominant mode and first higher order mode, the

resonant frequencies decreased with defection height increasing while resonant frequencies of second and third higher order modes have less variation. Moreover, the resonant frequencies of the first and second higher order modes are adjacent closely and at the same time they are far away from that of the dominant mode. This information served as a very useful idea to implement a wideband filter with multi-mode operation.

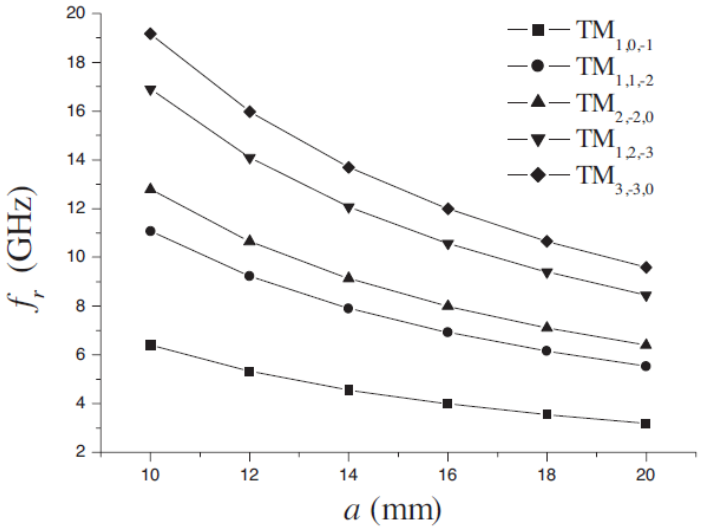

Figure 2.21: Relationship of resonant frequency and side length a(ε_r = 9.8, h= 0)

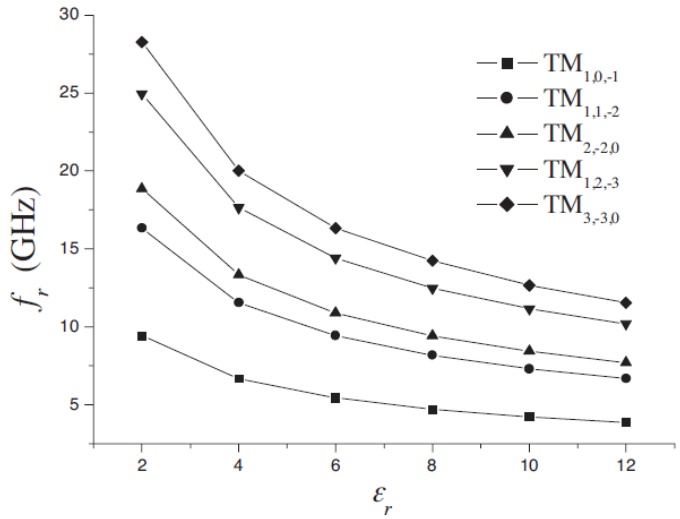

Figure 2.22: Relationship of frequency and dielectric constant (a = 15mm , h = 0)

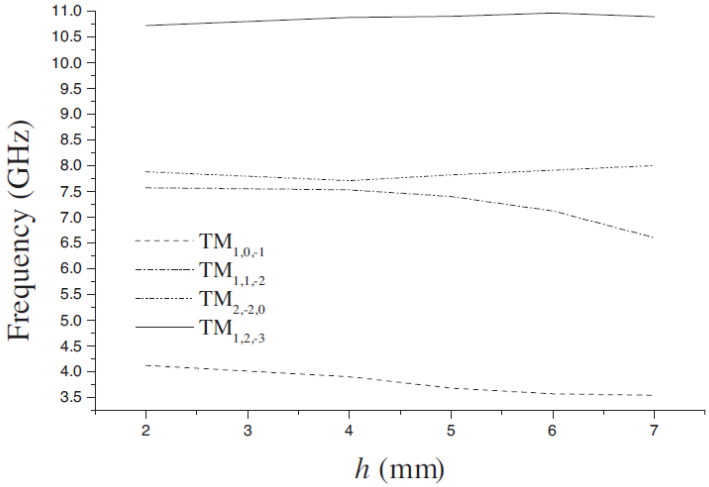

Figure 2.23: Relationship of defection height and resonant frequency for different resonant modes (ε_r = 9.8, a = 15mm, b = 8mm, d = 2mm)

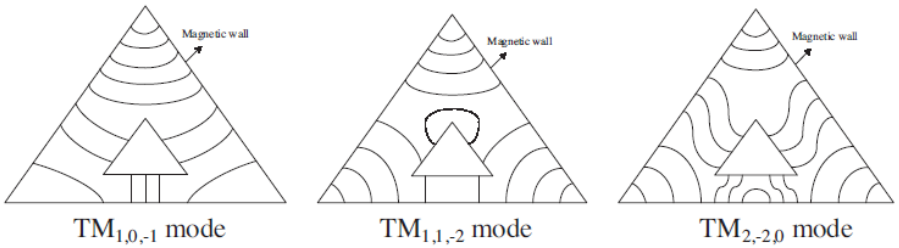

Figure 2.24: Magnetic field patterns of several resonant modes for an equilateral triangular patch resonator with one fractal shaped defection.

The basic principle of designing a microstrip filter is the selectivity and application of all sort of resonant modes. In this paper, fractal shaped defection act as perturbation element for a bandpass filter with multi-mode operation implementation. The required resonances of several higher order modes should be adjacent to each other for close coupling while resonance of the dominant mode should be possibly far away from these required resonances. A new multi-mode bandpass filter using equilateral triangular patch resonator with optimized parameters where a = 15mm, b = 8mm, h= 6mm and d = 1.75mm had been designed. The filter is designed on a Al_3O_2 ceramic substrate with relative dielectric constant of 9.8 and thickness of 1.27mm. The I/O feed lines that set at the edge of hemline are parallel microstrip lines with characteristic impedance of 50Ω is shown in Figure 2.25.

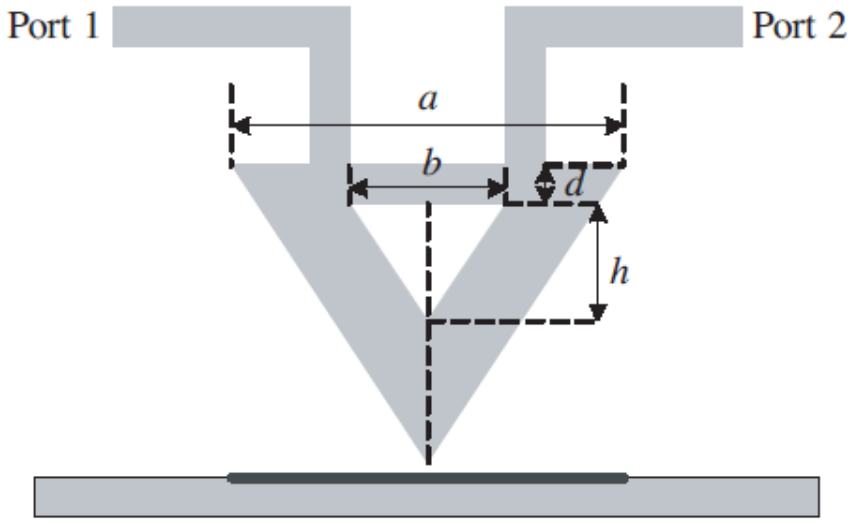

Figure 2.25: Microstrip equilateral triangular bandpass filter with fractal shaped defection.

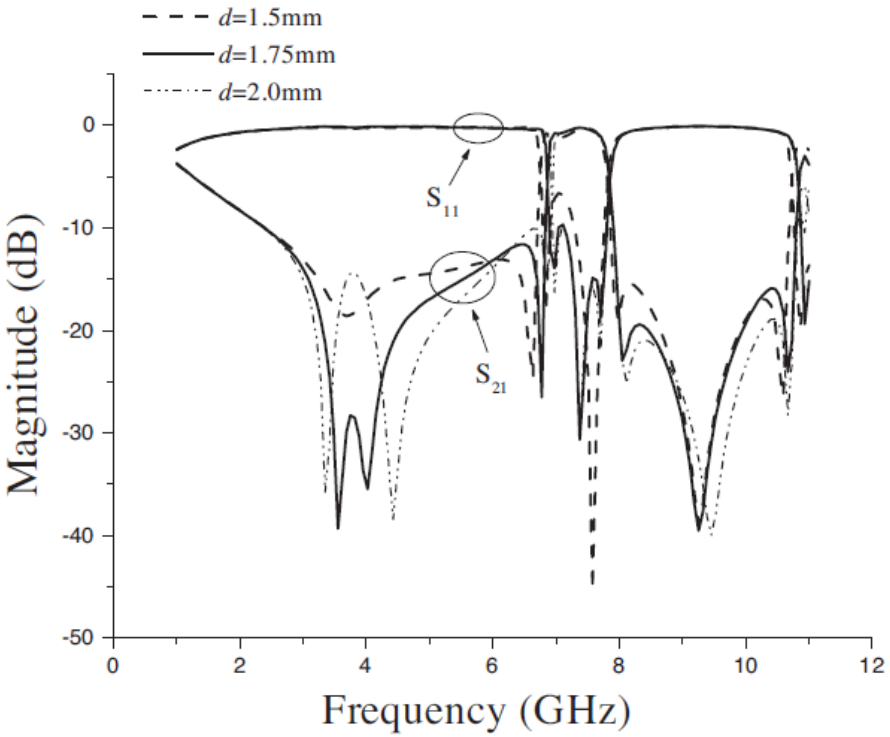

Figure 2.26: Simulated frequency response

From Figure 2.26, it can be seen that the filter has a wide stopband, multi transmission zeros at both sides of passband and lowpass insertion lost.

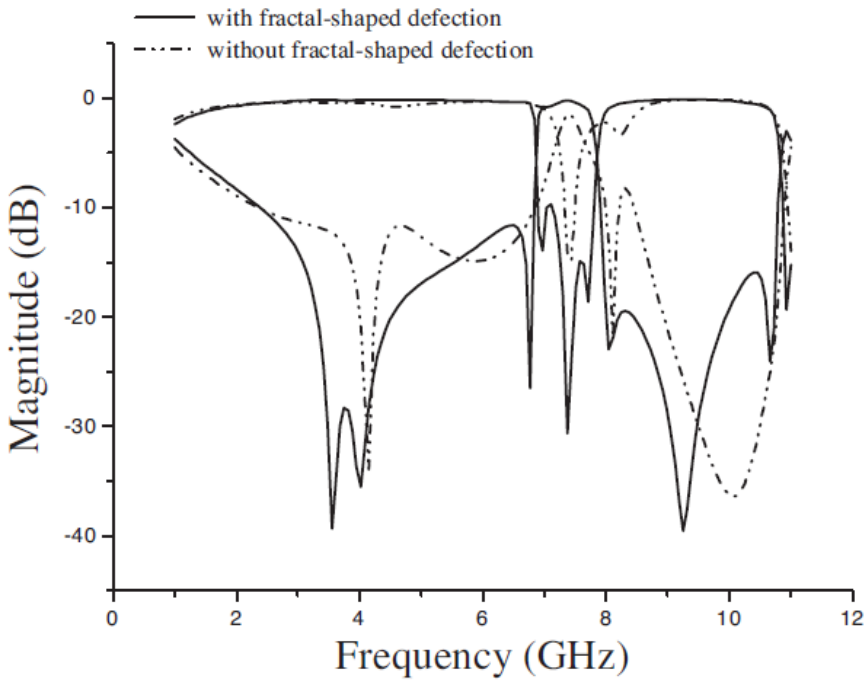

Figure 2.27: Comparison of frequency response (ε_r = 9.8, d = 1.75mm)

In this journal, the different ways for triangular patch resonator have been studied to introduce perturbation element. Fractal shaped defection was introduce to create a multi-mode bandpass filter. After studying the journal, it gave a very good idea on how to create a multi-mode bandpass filter.

2.2 Patch Filter

The rapid growth in wireless communications system such as mobile and satellite systems had boost up the research and development in microwave planar resonators because resonators are widely used in applications such as filters, antennas, circulators and oscillators. Microstrip patch resonators have advantages over coupled lines, rings and other type of resonators in bandpass filter application with lower insertion loss and high power handling capability. Lines resonators are less preferable because it suffer from higher conductor loss and lower power handling capability. Microstrip filters may be designed using single-mode or dual-mode resonators. Dual-mode microstrip filter have more attractive features such as

each resonator can behave as a doubly tuned resonant circuit and reducing by half the number of resonators required for a given filter. In this chapter, single-mode and dual-mode patch resonators will be discussed.

2.2.1 Applications of Patch Resonator

As mention before, patch resonators are more attractive compare to other resonators in terms of low insertion loss and high power handling capability. The only drawback of a patch resonator compared to other resonators is the size of the resonator which is slightly larger. Although patch resonators have a larger size, this drawback is not a big issue for the applications because the power handling or low loss has a higher priority. Furthermore, the size may not be a problem as the filters operate at very high frequencies. Patch resonators usually tend to have a stronger radiation due to high power handling capability. Filters are normally enclosed in a metal housing for filter applications so that the radiation loss can be minimized. Depending on the filter design requirements or applications, patch resonator may be designed in different shapes as shown in Figure 2.28. Nowadays, patch resonator filters are widely employed in wireless communication systems especially in mobile communication systems. For instance, Global System for Mobile (GSM) mobile phones are using dual-mode patch filter which just pass 900MHz and 1800MHz signal.

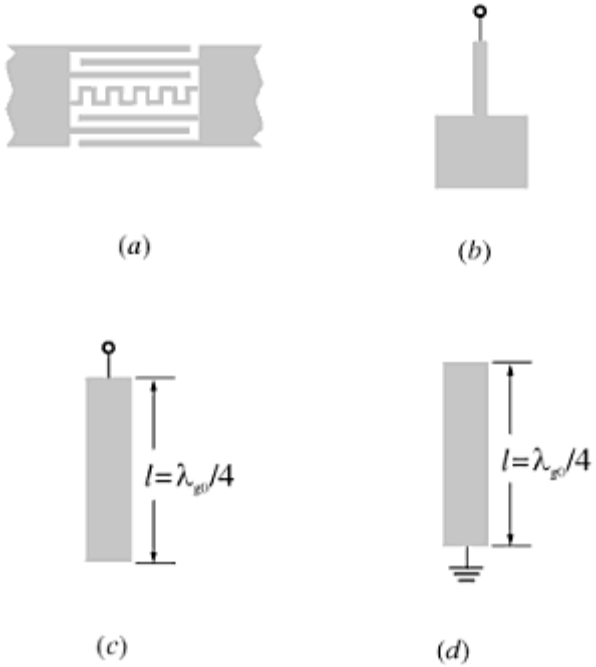

Figure 2.28: Variety shape of resonators

(a) Lumped-element resonator
(b) Quasi lumped-element resonator
(c) λ/4 resonator (Shunt series resonance)
(d) λ/4 resonator (Shunt parallel resonance)

2.2.2 Single-Mode Patch Filter

Single-mode microstrip filter is not highly preferable in filter design due to the narrow band characteristic. Dual-mode filter is more preferable due to the wider band and the features it provides. Furthermore, modification can be done on most of the single-mode filter to change to a dual-mode filter by introduction of stubs or slots.

In "New Compact Microstrip-Patch Bandpass Filter with Two Transmission Zeros" from Xuedong Wang and Jie Zou, a novel triangular patch filter has been design with single mode characteristic. The novelty of the filter design is two transmission zeros characteristic which can improve the selectivity and efficiency of spectrum utilization. Figure 2.29 shows the configuration of the filter design and Figure 2.30 shows the frequency response of the proposed filter. From Figure 2.30,

when W is equal to 2 mm, the frequency response of the returned loss is a single-mode. As the width of W is increased the S_{11} frequency response is improved.

This design will just serve as reference on designing a filter because the requirement of the project is dual-mode filter. Furthermore, triangular shape is more difficult to design compared to rectangular shape. The simplicity of the filter can be adapted into the project.

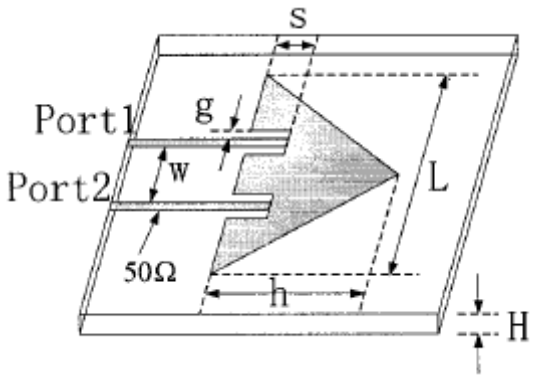

Figure 2.29: Configurations of single-mode triangular patch filter

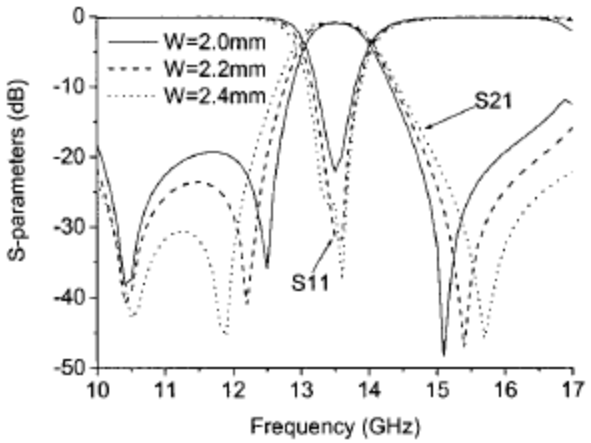

Figure 2.30: Single-mode Response

2.2.3 Dual-Mode Patch Filter

A planar dual-mode filter was proposed in the early 1970's by Wolff. Recently dual- mode bandpass filter has gained popularity in designing filter. There

are many dual-mode filter structures which have been proposed. However due to high coupling loss between feed line and resonator, their application is narrow down. In this paper with the tile “Compact and Low Insertion Loss Dual Mode Bandpass Filter” by Y.Sung is reviewed. The proposed filter provides low insertion loss because there is no coupling gap and radiation loss in feed structure. The impedance matching can be easily obtained without the coupling gap between feed line and patch resonator.

A compact dual-mode filter with crossed slots and spur lines is proposed in the article. Gap on the feed line is removed by mounting L-type spur line to the conventional dual-mode filter with crossed slots. Square patch resonator possessing cross-slots and spur lines as a form of perturbation is focus in the article. The proposed filter uses patch resonator with a pair of crossed slots on the conductor surface leads to a several advantageous features such as effective size reduction, radiation loss reduction and easy mode coupling. Figure 2.31 shows the conventional and proposed dual-mode filter configuration. On the filter, L-type spur line is incorporated into a side of the square patch for exciting and coupling a pair of degenerate modes.

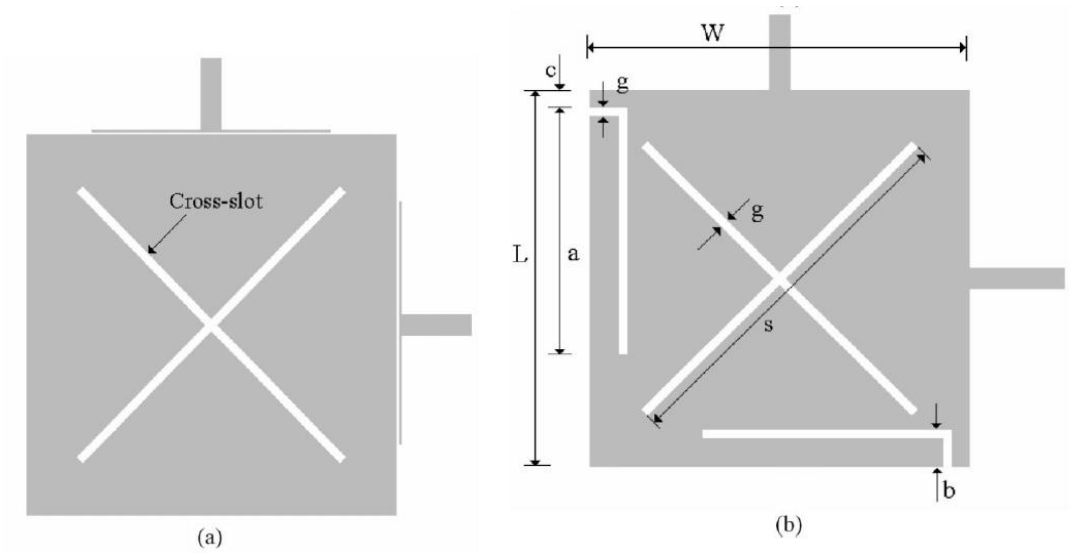

Figure 2.31: (a) Conventional dual-mode filter with the crossed slots, (b) Proposed dual-mode filter with the crossed slots and spur lines

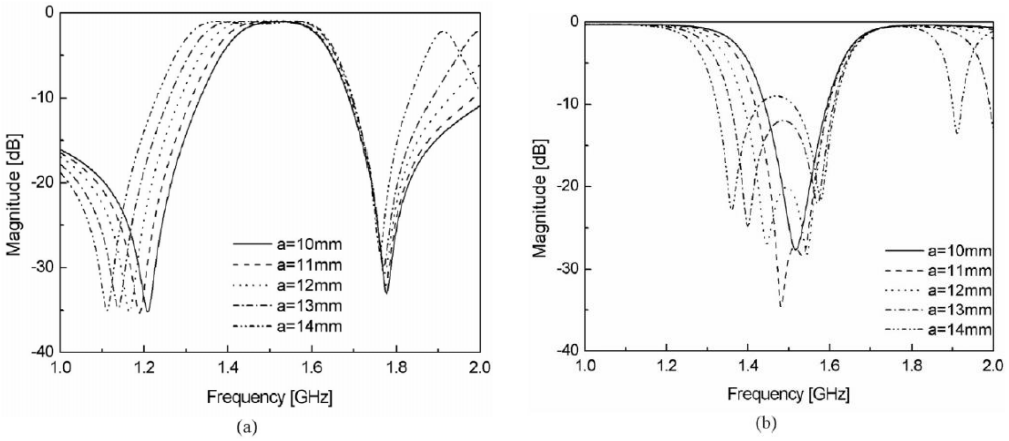

Figure 2.32: Simulation result of dual-mode filter with different lengths a,
(a) Insertion loss. (b) Returned loss

The characteristic of the dual-mode filter is analyzed and is shown on Figure 2.32 - Figure 2.35. Figure 2.32 shows the insertion loss and return loss of different length a of spur lines. It can be observed that when a = 10mm there is no perturbation on square patch and only single mode is excited. It can be said that the longer the length a, the stronger the coupling happened. The proposed design has wider range than conventional structure in term of size of perturbation because two identical structures are used by the same substrate in the same frequency band. This also means that the proposed filter will reduce the uncertainty during fabrication because the coupling gap is not introduced. The changes in the length also change the attenuation pole. The attenuation pole can be tuned by adjusting the length of the spur lines.

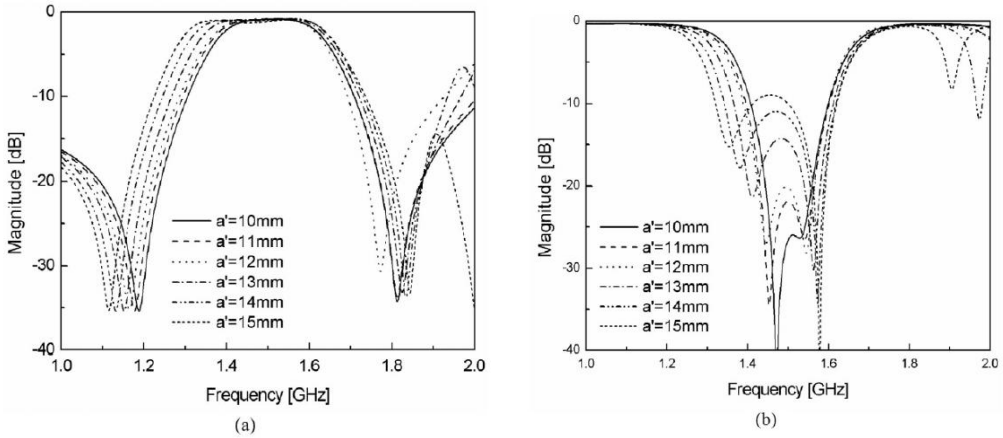

Figure 2.33: Simulation result of dual-mode filter with different lengths a'
(a) Insertion loss. (b) Returned loss

In Figure 2.33, the insertion loss and returned loss of unsymmetrical spur lines is shown. One of the spur line is fixed at the length of a = 12mm x b = 2mm while another side a' is changing from 10mm to 15mm with fixed b = 2mm. The simulated results show that the unsymmetrical spur lines filter also produces the characteristic of dual-mode. The coupling range of unsymmetrical spur lines is broader than symmetrical spur lines. In Figure 2.34, by changing the width b of the spur lines, the mode splitting is affected as same in changing the length of the spur line. When the width b is less than 1.8mm, there is no evidence of mode splitting. The resonant frequency of the splitting mode increases when the width of the spur lines increases. This implies that the longer the perturbation length, the stronger the coupling between orthogonal modes. The changes of resonant frequency with different width b is similar to the changes of resonant frequency with the length a. The attenuation pole is also affected by the spur lines width.

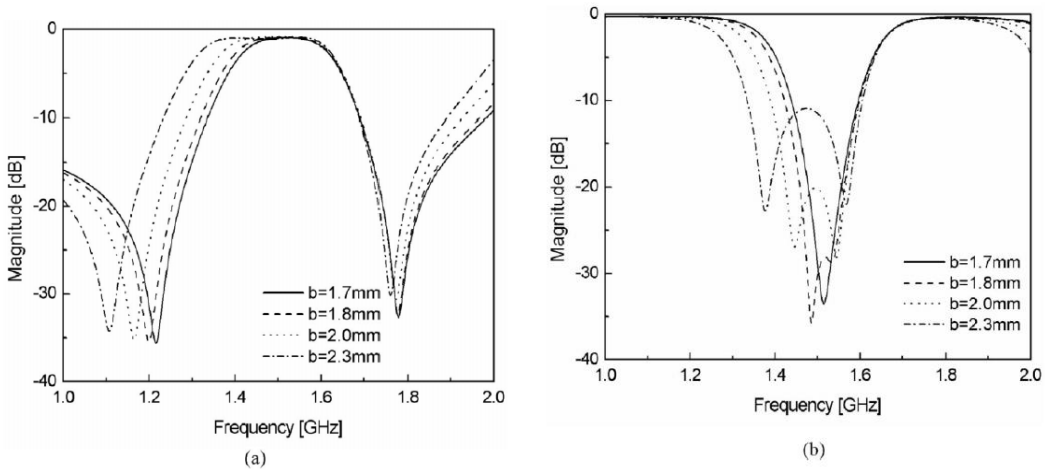

Figure 2.34: Simulation result of dual-mode filter with different width b
(a) Insertion loss. (b) Returned loss

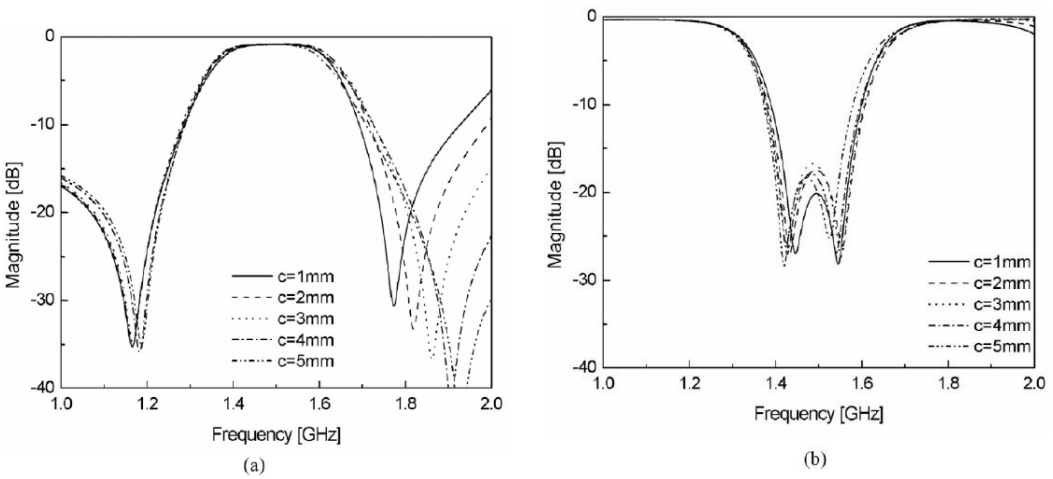

Figure 2.35: Simulation result of dual-mode filter with different position c
(a) Insertion loss. (b) Returned loss

It can be observed from Figure 2.35 that the variation of position c does not give a significant variation on the resonant frequency and also the attenuation pole. Figure 2.36 shows the simulated and measured frequency response of the fabricated filter. The measured minimum insertion loss is -0.9dB with greater than -10dB of returned loss in the passband range. The loss is mainly due to the conductor and electrical loss. From this article, it is understood that a cross-slot is utilized to produce a low insertion loss of a dual-mode filter. After studying this paper, the understanding of the method used to design a low loss dual-mode filter and also the cross-slot functionality is increased. The idea of this paper can be used as reference in this project.

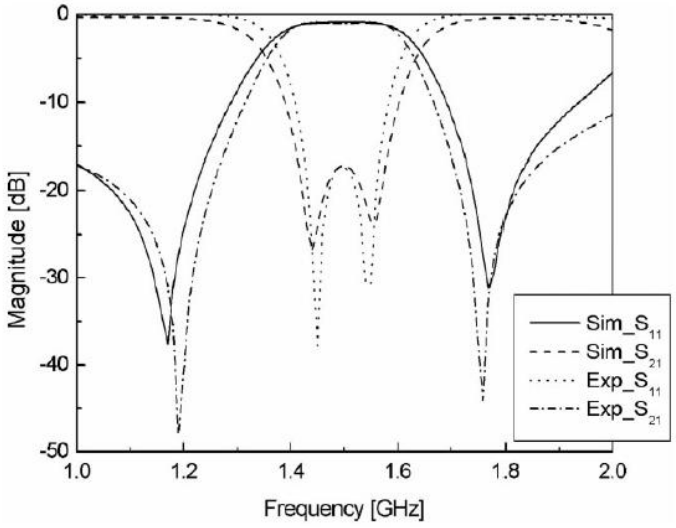

Figure 2.36: Simulated and measured frequency response of proposed filter

CHAPTER 3

MICROSTRIP PATCH BALUN BANDPASS FILTER

3.1 Background

The fundamental design of microstrip patch balun bandpass filter is based on the journal published in IEEE Transactions On Microwave Theory and Techniques, Vol. 47, No. 5, May 1999 with the title "New Planar Dual-Mode Filter Using Cross-Slotted Patch Resonator for Simultaneous Size and Loss Reduction" by Lei Zhu, Pierre-Marie Wecowski, and Ke Wu. The novelty of structure shown in Figure 3.1 used a pair of unequal crossed slots that are formed on a square patch resonator such that its radiation loss and structure size can be significantly reduced simultaneously.

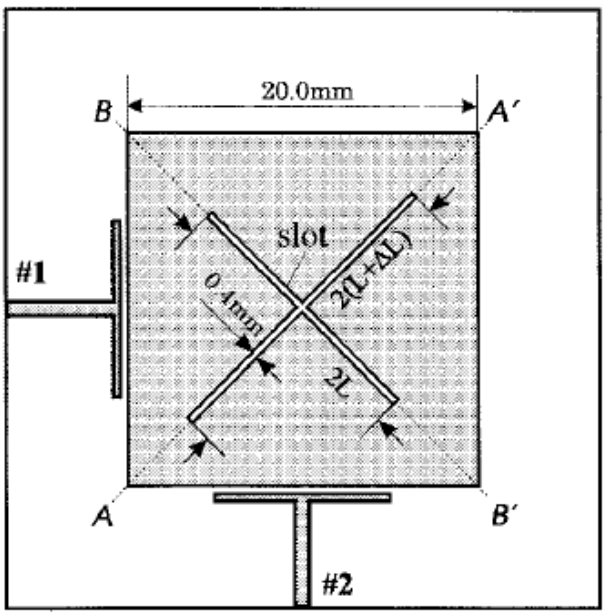

Figure 3.1: Filter layout

The planar dual-mode filter is designed with ground plane and substrate on top etched as shown of Figure 3.1. The thickness of the substrate is 1.27mm. The dimension of the square patch is 20 x 20 mm^2. The crossed slot is etched out with unequal length of L with the differences ΔL where L = 10.2mm and ΔL = 0.17mm. Figure 3.2 and Figure 3.3 show a comparison of a predicted and measured frequency response for an optimized design example of the proposed dual-mode filter with the cross-slots. The mechanical tolerance of ± 1mil allowed by the MIC fabrication facilities is considered for the design prediction in relation with the ideal case.

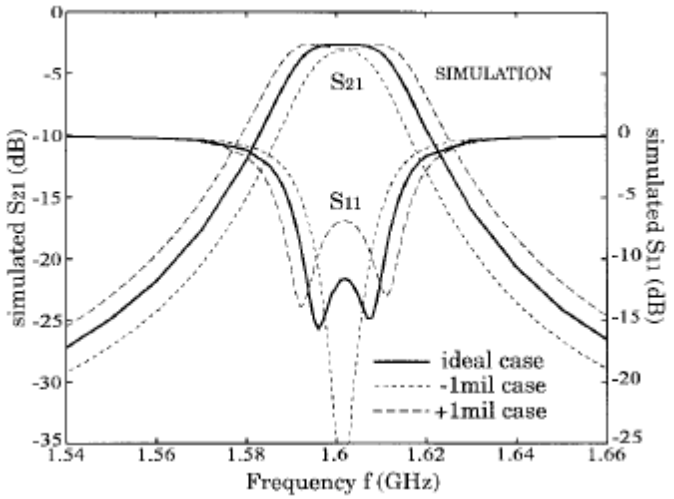

Figure 3.2: Simulated results

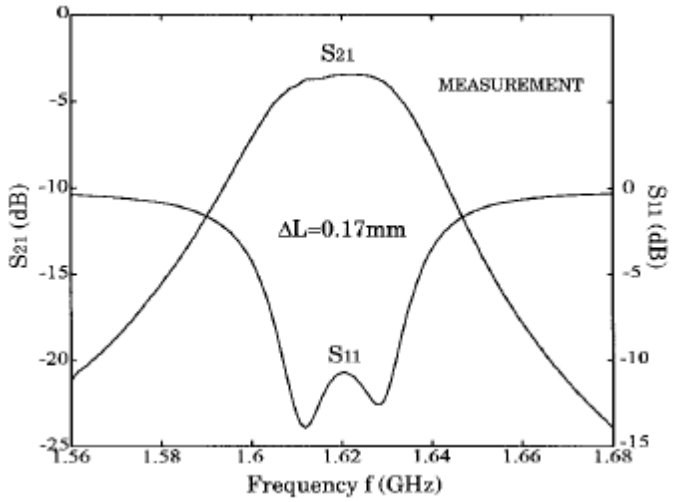

Figure 3.3: Measured results

3.2 Research Methodology

Throughout the process of designing and fabricating the filter, the author has encountered various obstacles and problems in this project. The filter design procedures will be discussed in this chapter on the simulation stage, fabrication stage and experimental stage. Each of the stage mention above has its own difficulty and play an important role towards the success of this project.

3.2.1 Simulation Stage

After studying the journals that obtained from the IEEE Xplore database, a few tutorials have been gone through by the author to familiarise with the High Frequency Structure Simulator (HFSS) software. The tutorials are easy to understand as there are step by step instructions that guide the user on how to use the software. In addition, there is a help menu that will direct user to an online webpage to learn in more detail. Next, a journal had been chosen by the supervisor and the author is required to repeat the journal by using High Frequency Structure Simulator (HFSS) software. This step is to ensure that the author had really understand and able to carry out simulation without any guidance. The simulated result by the author is similar to the results on the journal. There are slight variations on the simulated results by the author compare to the journal due to the different simulation software that has been used. However, the supervisor had confirmed that the simulated results are acceptable and the author is able to carry on to the designing stage. The whole process of learning the software took a period of 1 week.

The characteristic impedance Z_o is playing an important role in microstrip lines design which will affects the reflection loss, S_{11}. Hence, a 50 ohm of characteristic impedance feed line has been formed to achieve the impedance matching. The characteristic impedance of feed line is calculated using TX Line 2003 software. The width that generated by using this software that produce a 50 ohm feed line on RT/Duroid 6006 with the dielectric constant of 6.15 and thickness of the substrate of 0.635mm is 0.933mm.

Designing stage had been carried out on rectangular patch with one input and 2 outputs configuration. The first configuration did not produce the desired results hence modifications have been done on the design for several times before getting the final configuration which is workable and produce the desire result. Modifications that had been done include the change of the configuration and the dimension. Figure 3.4 shows a few configurations of the filter designs which did not produce the desired results.

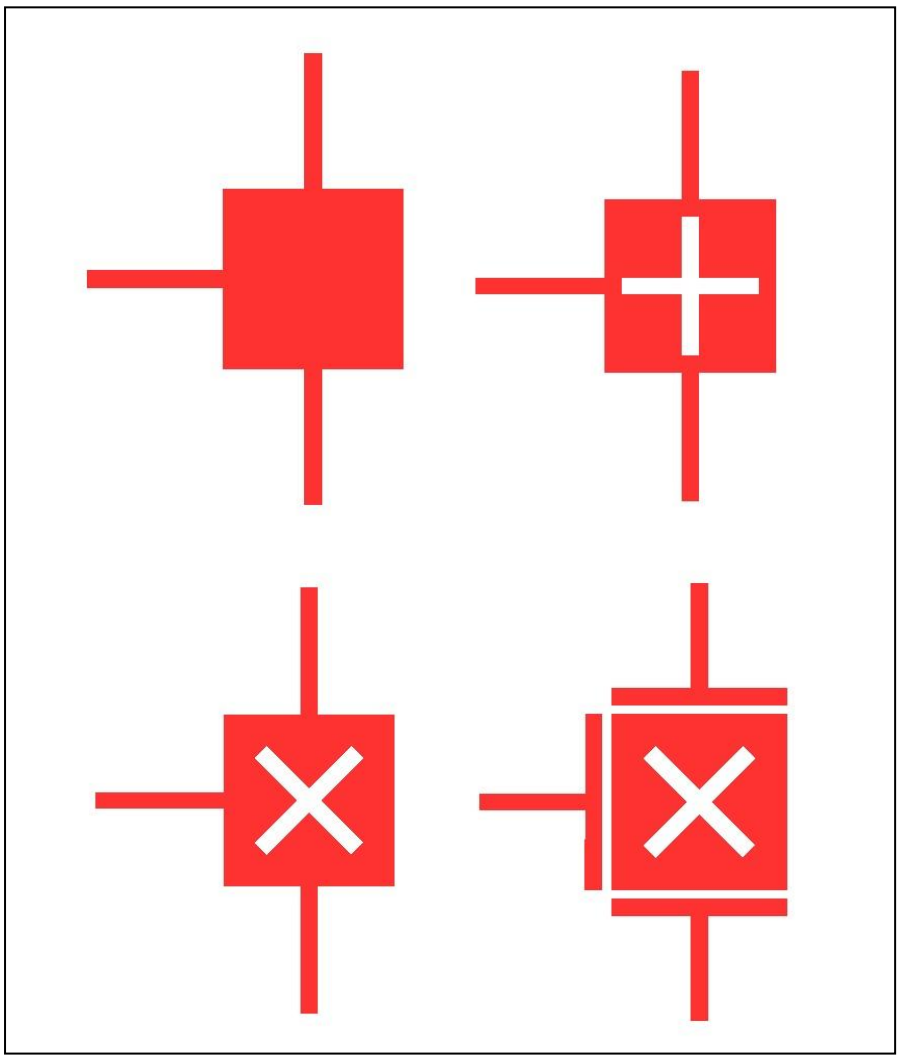

Figure 3.4: Configuration that does not work

The simulation stage is the toughest stage and it took a lot of time and patience to do the simulation during designing stage of the filter. Each simulation took a period of time ranging from half an hour to one and half hour for a complicated design. Simulation duration is dependent on the complexity of the

design and the computer processing speed. While waiting for the simulation results to be done, the author did some analysis on previous results and modifications on the design for next simulation. Modification and improvement can be easily done on the design base on the analysis of previous results. The simulation stage took two months to complete before going into the fabrication stage. Throughout the simulation stage, perseverance and patience are very important to get the author keep trying until a new filter design is successfully simulated with good performance.

3.2.2 Fabrication Stage

The optimized simulation results had been sent to the supervisor for verification before the fabrication process start. RT/Duroid 6006 substrate is used to fabricate the filter. RT/Duroid 6006 microwaves laminates are ceramic polytetrafluoroethylene (PTFE) composites which are designed for electronic and microwave circuit applications that require a high dielectric constant. PTFE is most well known by the DuPont brand name Teflon. Moreover PTFE is a fluorocarbon solid, as it is a high-molecular weight compound consisting only of carbon and fluorine which make PTFE hydrophobic. This property of PTFE is suitable for the fabrication process because during the fabrication, the substrate is highly exposed to water. PTFE has one of the lowest coefficients of friction against any solid.

RT/Duroid 6006 is available with dielectric constant value of 6.15. In addition, RT/Duroid 6006 features ease of fabrication and stability in use. It might have tight dielectric constant and thickness control, low moisture absorption and good thermal mechanical stability. RT/Duroid 6006 laminates are supplied with clad both sides ¼ oz to 2 oz / ft^2 (9 to 70 µm) electrodeposited copper foil.

The first step of the fabrication process is to draw the filter design configuration with exact dimension using Easily Applicable Graphical Layout Editor (EAGLE) software from CadSoft. The size of filter that printed out must be 100%

exactly of the size of the simulation filter design. The gap for capacitive coupling is extremely sensitive for this design. A 0.01mm mismatch may affect the final result tremendously. Next, the ready design is printed on a special waterproof inkjet film shown in Figure 3.5. The film has different types of surface on both sides where one side of the surface is smooth while the other side has a sticky surface. The design must be printed on the sticky surface and must avoid touching the area of the printed design. An example of the printed design on the film is shown in Figure 3.6.

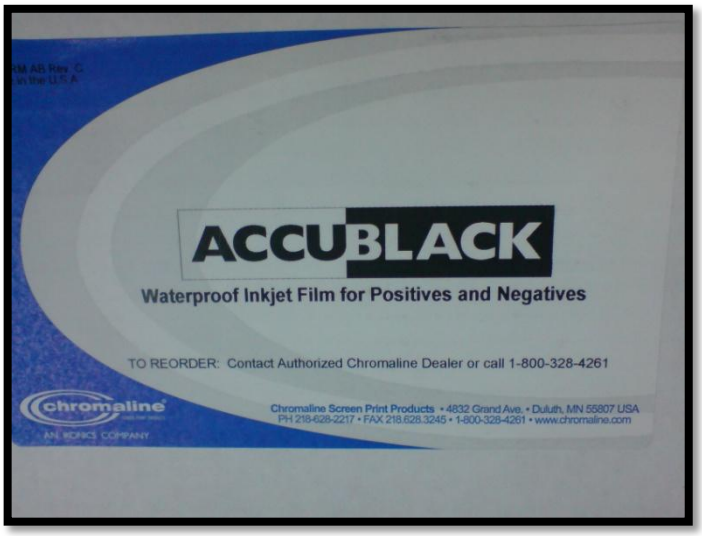

Figure 3.5: Box cover of ACCUBLACK waterproof inkjet film

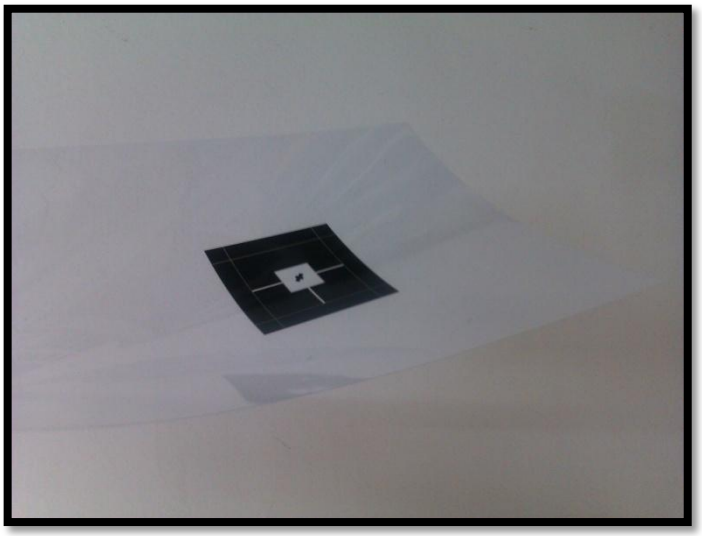

Figure 3.6: Ready printed design on the film

Before printing the design, there are some basic settings that have to be set in the EAGLE software. In EAGLE software, the file that export the format “BITMAP”

should set to the highest resolution to ensure the separated gap is clearly printed. Without high resolution image the gap might be blur and the rectangular patch resonator and the feeding line might be connected partially. The image must be inverted before the filter design is print on the film because the RT/Duroid 6006 substrate is of negative photoresist properties.

The size of the substrate is cut slightly larger than the size of the filter design to provide adequate space for cutting at the end of the fabrication process. The substrate that had been cut is placed on top of a hard cardboard. Then a thin layer of ultraviolet (UV) plastic film is placed on top of the substrate and slowly rolled into the laminating machine to be laminated. The temperature of the laminate machine is set to be 140 ºC. Both side of the substrate need to be laminate with UV plastic film so that the thin layer of the copper foil will not etch away during the etching process. Next, the printed design of the filter film is placed on top of the laminated substrate with the sticky surface facing down. Hence, it is put into the UV exposure machine to expose with UV light for approximately 15 seconds. The duration of the exposure must not be too short or too long according to the advice from Mr. Ho.

After it has been exposed with UV light, the substrate is washed with sodium hydroxide (NaOH). This step must be done carefully and in very detail because the area of the etching is based on it. Fine brush is used to brush off the dark colour for the fine gap such as the capacitively coupling gap. This step is completed when all the dark colour on the substrate is wash off. The substrate is put on a tray to let it dry for about 1 to 2 hours. Next, the substrate is put inside the etching machine containing liquid ferric chloride at the temperature of 45 ºC. The substrate must not be soaked directly into the liquid ferric chloride because it will over etch the area. Hence, the soaking technique is very important in order not to miss out or over etch some of the areas of the substrate. The last part of the fabrication process is to wash away the remaining of UV film on the substrate by using potassium carbonate (K_2CO_3).

In order to take measurement on the design filter, connectors are place on each port of the filter. The connector is soldered to the feed line of the port using soldering iron. During the soldering process, the ground plane and the feeding line

must not be connected to each other to avoid short circuit. Figure 3.7 – Figure 3.10 show the equipments that are used during the fabrication process.

Figure 3.7: Laminating machine

Figure 3.8: Exposure machine

Figure 3.9: Sodium hydroxide (NaOH)

Figure 3.10: Potassium carbonate (K_2CO_3).

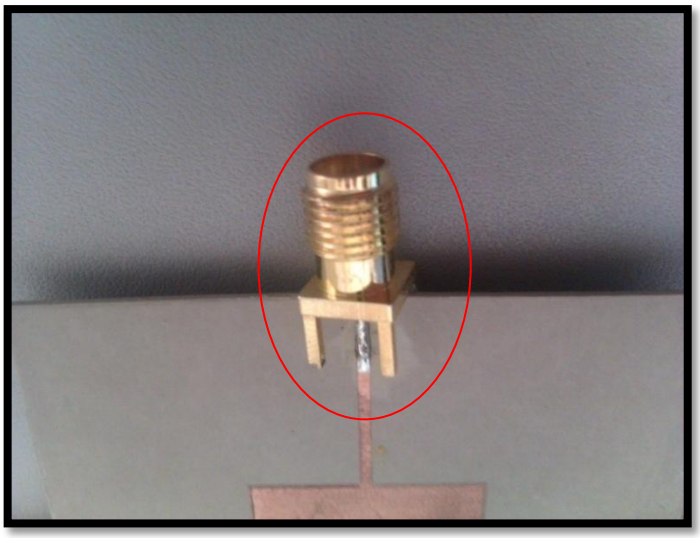

Figure 3.11: Connector

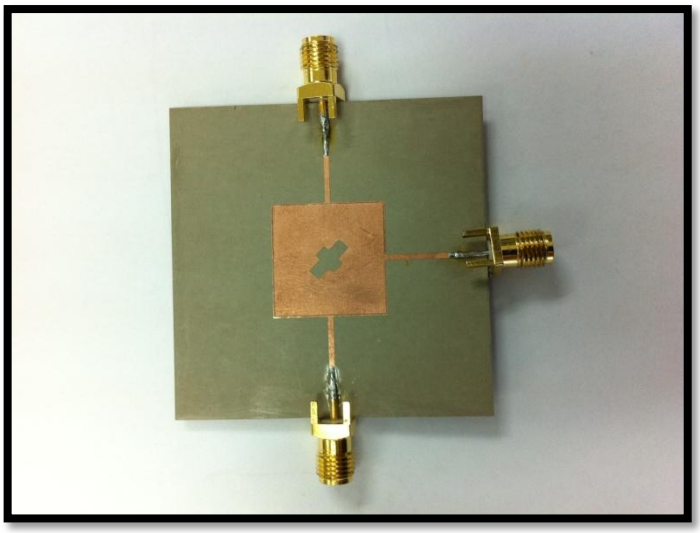

Figure 3.12: Fabricated filter

3.2.3 Experimental Stage

The experimental stage is the last stage in the research methodology. This stage is very important as it determines the success of the whole research and project. The simulation results are compared to the measured results to validate the workability of the filter. In this stage, the filter is measured using Rohde & Schwarz ZVB8 Vector Network Analyzer (VNA). The measurable frequency range of the VNA is between 300 kHz to 8 GHz. This filter design have a frequency range is

between 1 GHz to 6GH hence the limitation of the measuring equipment is not an issue where the experiment still can be carried out.

Figure 3.13: Rohde & Schwarz ZVB8 Vector Network Analyzer (VNA)

Before the measurement is carried out, the VNA need to be calibrated to eliminate the signal loss and phase shift introduced by the cable during measurement. The VNA able to self adjust on the S-parameters after the calibration process. As shown in Figure 3.14, there are total of five ports with each of them having different function of calibration. First of all, port 1 of the VNA is connected to "Open" follow by "Short" and "Match". This step is repeated with port 2 of the VNA. Next step is to connect port 1 and port 2 of the VNA to the calibration tool simultaneously through the port "Thru".

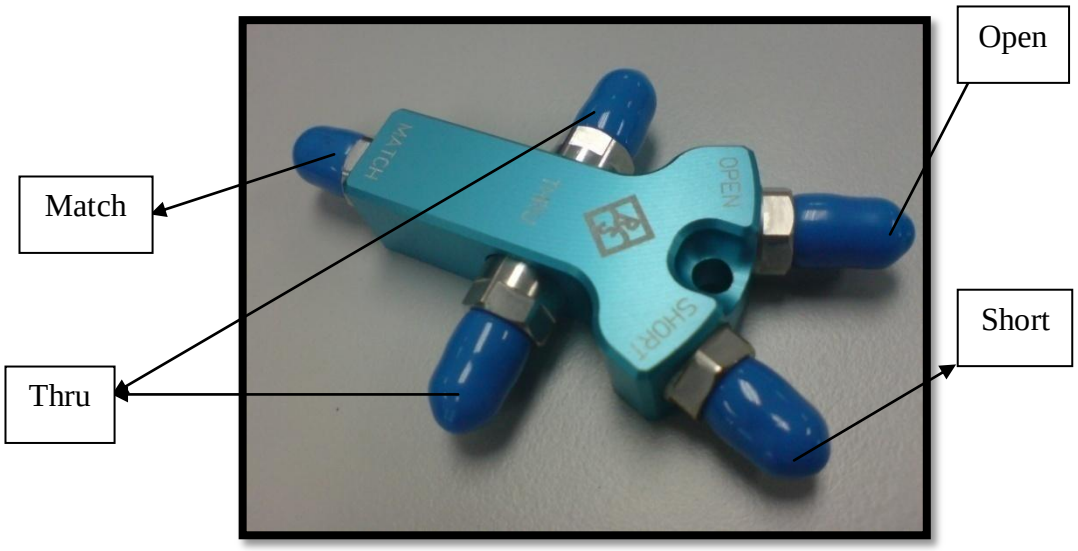

Figure 3.14: Rohde & Schwarz Calibration Tool Kit

Hence the experiment can be carried out after the calibration is done. There are 3 ports in the filter design but the VNA is available with 2 ports. In order to measure the results, port 2 and port 3 of the filter need to be measure separately. This can be done by using a match shown in Figure 3.15. Port 1 and port 2 of the filter were connected to the VNA while port 3 of the filter were connected using the match. Figure 3.16 shows how the filter is connected to the VNA. This configuration of the connection is to measure the insertion lost of port 2 as port 3 is match. The above step is repeated where port 2 is match while the insertion lost of port 3 is measured. The frequency range and sweep point need to be adjusted in order to get a result similar to the simulation result. Figure 3.17 shows a pair of cable used to measure the results. The results are saved to compare to the simulated results.

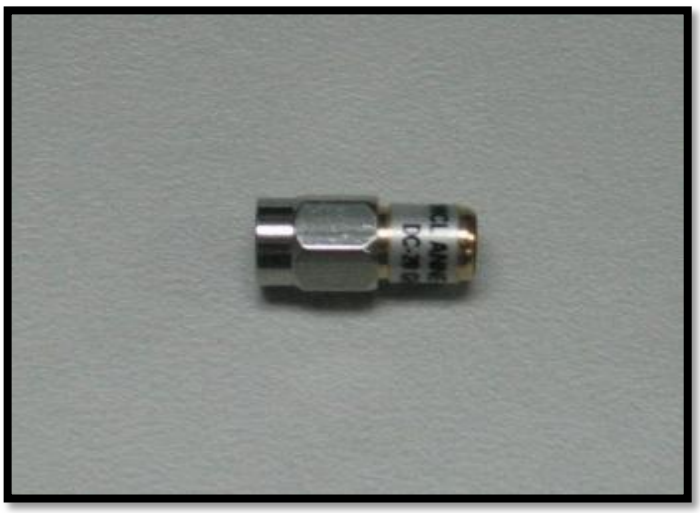

Figure 3.15: Match

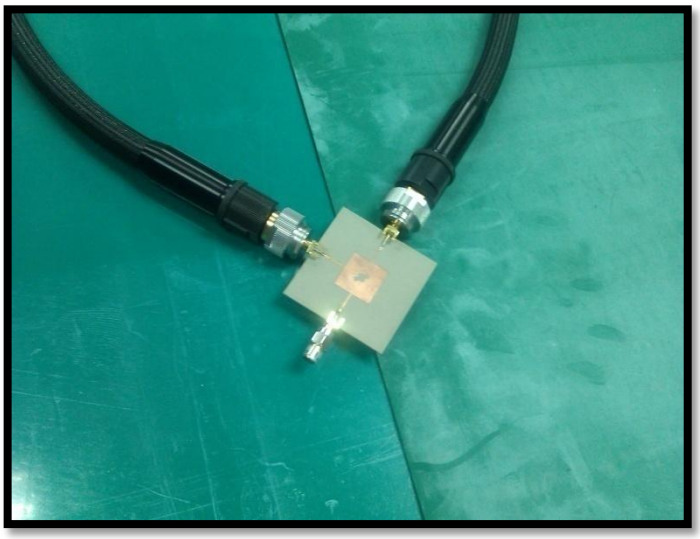

Figure 3.16: Filter connected to VNA using cable

Figure 3.17: Cable

3.3 Proposed Filter Configurations

A microstrip patch balun bandpass filter has been designed based on the Dual-Mode Filter Using Cross-Slotted Patch Resonator as been discussed above. The proposed design configuration is shown in Figure 3.18. The patch filter is formed by using unequal cross-slot etched out from the rectangular patch to produce a dual-mode patch balun filter. The cross-slot is rotate with the angle of 45 degree from the horizontal to obtain two degenerate modes. Port 1 is the input signal where the feeding line is directly coupled to the rectangular patch. Port 2 and Port 3 is the output signal where the feeding lines of Port 2 and Port 3 are capacitively coupled to the rectangular patch to produce the desired bandwidth of the filter. The ground plane is fully consists of thin film copper without any etching on the surface.

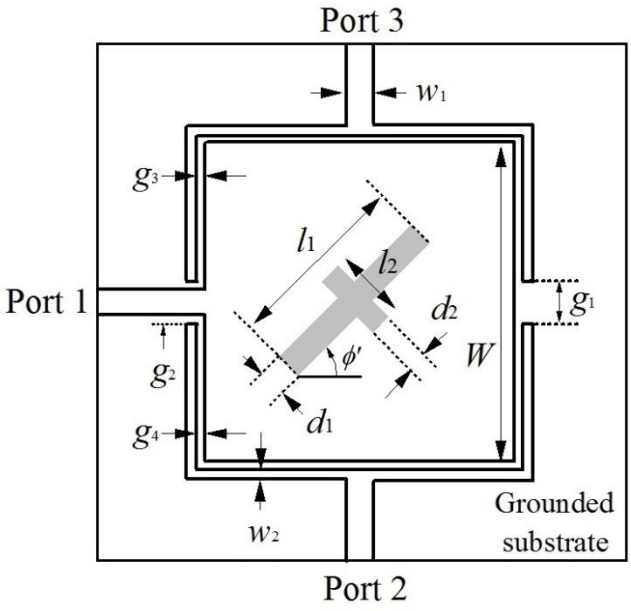

Figure 3.18: Top view of configuration of the proposed microstrip patch balun filter. Dimensions of the filter: W = 18 mm, w_1 = 0.933 mm, w_2 = 0.2 mm, g_1 = 0.2 mm, g_2 = 0.1335 mm, g_3 = 0.1 mm, g_4 = 0.07 mm. l_1 = 7 mm, l_2 = 4 mm, d_1 = 2mm, d_2 = 2mm and ϕ' = 45^0

The substrate used is Duroid 6006 which has a dielectric constant of ε_r = 6.15 with a thickness, H = 0.635 mm and the size of the substrate is 50.0 mm(W) × 50.0 mm(W). The microstrip feed line that connected to Port 1, Port 2 and Port 3 is of width w_1 = 0.933mm which is 50ohm impedance matching. The capacitive coupling gap is set to be as narrow as possible to obtain a result that is similar without coupling gap and at the same time give a desired bandwidth. The optimal microstrip patch balun bandpass filter parameters are taken as W = 18 mm, w_1 = 0.933 mm, w_2 = 0.2 mm, g_1 = 0.2 mm, g_2 = 0.1335 mm, g_3 = 0.1 mm, g_4 = 0.07 mm. l_1 = 7 mm, l_2 = 4 mm, d_1 = 2mm, d_2 = 2mm and ϕ' = 45^0 based on the simulation results of High Frequency Structure Simulator, HFSS. Generally, the basic design concept is taken from Lei Zhu, Pierre-Marie Wecowski, and Ke Wu papers on dual-mode filter using cross-slotted patch resonator design.

CHAPTER 4

RESULTS AND DISCUSSIONS

4.1 Simulation and Experimental Results

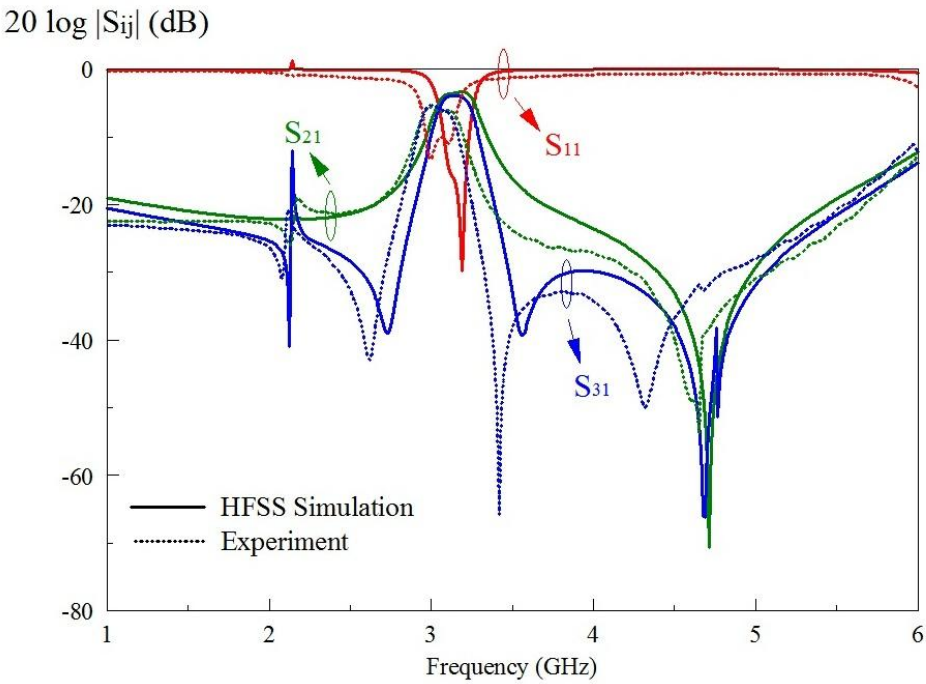

Figure 4.1: Frequency response of simulated and measured S parameters of the microstrip patch balun filter

Throughout the entire project, all the simulations are done by using High Frequency Structure Simulator (HFSS) software while all the measurements are done by using Rohde & Schwarz Vector Network Analyzer ZVB8. Figure 4.1 shows a comparison of simulated and measured S parameters with respect to the frequency.

This frequency response of S parameters not only shows that the filter is a bandpass filter but also function as a balun at the same time.

With reference to Figure 4.1, a reasonable good agreement is found in between the simulated and measured frequency response. The passband center frequency of both S_{21} and S_{31} is at 3.05 Ghz with passband covering between 2.91 – 3.19 GHz. Two transmission zeroes are also observed in S_{31} near to the filter passband. On the other hand the output signal magnitudes $|S_{21}|$ and $|S_{31}|$ are equal and read at -6 dB. This might due to additional losses that introduced by the connectors and feed lines. Figure 4.2 gives the measured output phase different of the microstrip patch balun filter. The phase bandwidth is approximately (180 ± 5^0) at the frequency range of 2.86 – 3.4 GHz. The insertion loss of the filter had clearly shown a dual-mode characteristic.

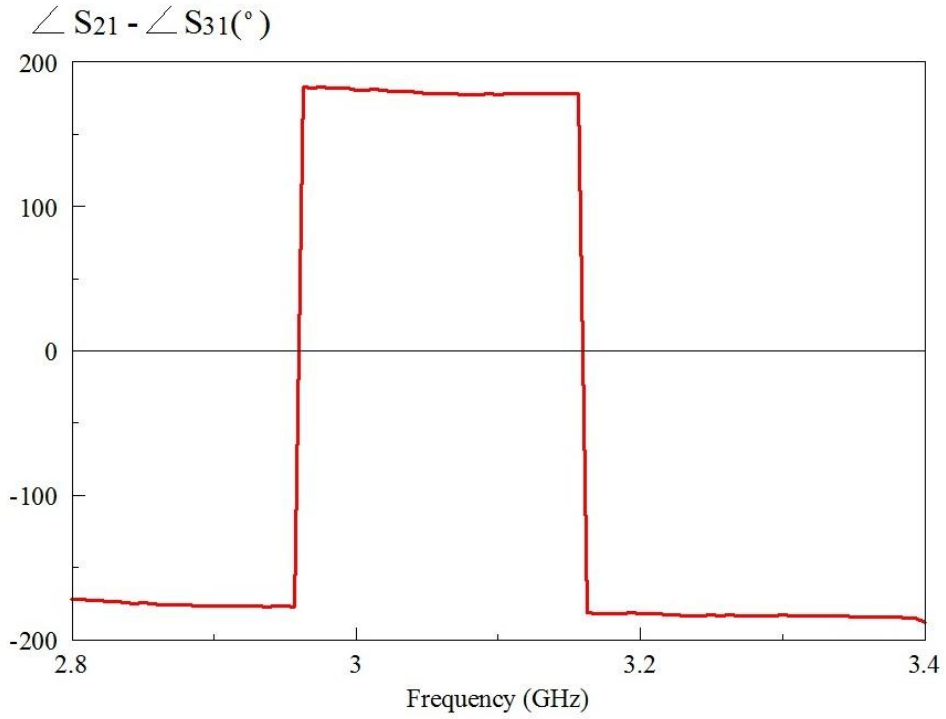

Figure 4.2: Measured output phase different of the microstrip patch balun bandpass filter at inclination angle of 45°

	S_{21}		S_{31}	
	Simulation	Experiment	Simulation	Experiment
Highest point(dB)	-3.3629320	-5.62	-3.9125882	-5.33
Reference(dB)	-6.3629320	-8.62	-6.9125882	-8.33
f_L(GHz)	3.01875	2.91875	3.03125	2.93125
f_H(GHz)	3.2875	3.18125	3.25625	3.14375
f_C(GHz)	3.153125	3.05	3.14375	3.0375
Amplitude bandwidth (%)	8.523	8.607	7.157	6.996
f_{LP}(GHz)	3.125	2.96	3.11875	3.155
f_{HP}(GHz)	3.1375	2.96	3.13125	3.17
f_{CP}(GHz)	3.13125	2.96	3.125	3.1625
Angular Bandwidth (%)	0.399	0	0.4	0.474
Error (%)	3.27		3.38	

Table 4.1

Table 4.1 shows the calculated value for the center frequency, percentage of amplitude and angular bandwidth and also percentage error between simulated and measured center frequency. The formula for calculating the center frequency, amplitude bandwidth and angular bandwidth is shown below with a figure as reference. $f_H \; and \; f_L$ is the high cut off frequency and low cut off frequency respectively. Figure 4.3 and Figure 4.4 show the phase angle of the simulated and measured S_{21} and S_{31} parameters respectively. Both give a reasonably and good agreement on the phase angle to support the calculated phase bandwidth of approximately (180 ± 5^0) which encompasses 2.86 – 3.4 GHz.

Center frequency, $f_c = \frac{f_H + f_L}{2}$

Amplitude bandwidth $= \frac{f_H - f_L}{f_C} \; x \; 100\%$

Angular bandwidth $= \frac{f_{HP} - f_{LP}}{f_{CP}} \; x \; 100\%$

$$\text{Error} = \frac{f_{c(simulated\ )} - f_{c(experiment\ )}}{f_{c(simulated\ )}}\ x\ 100\%$$

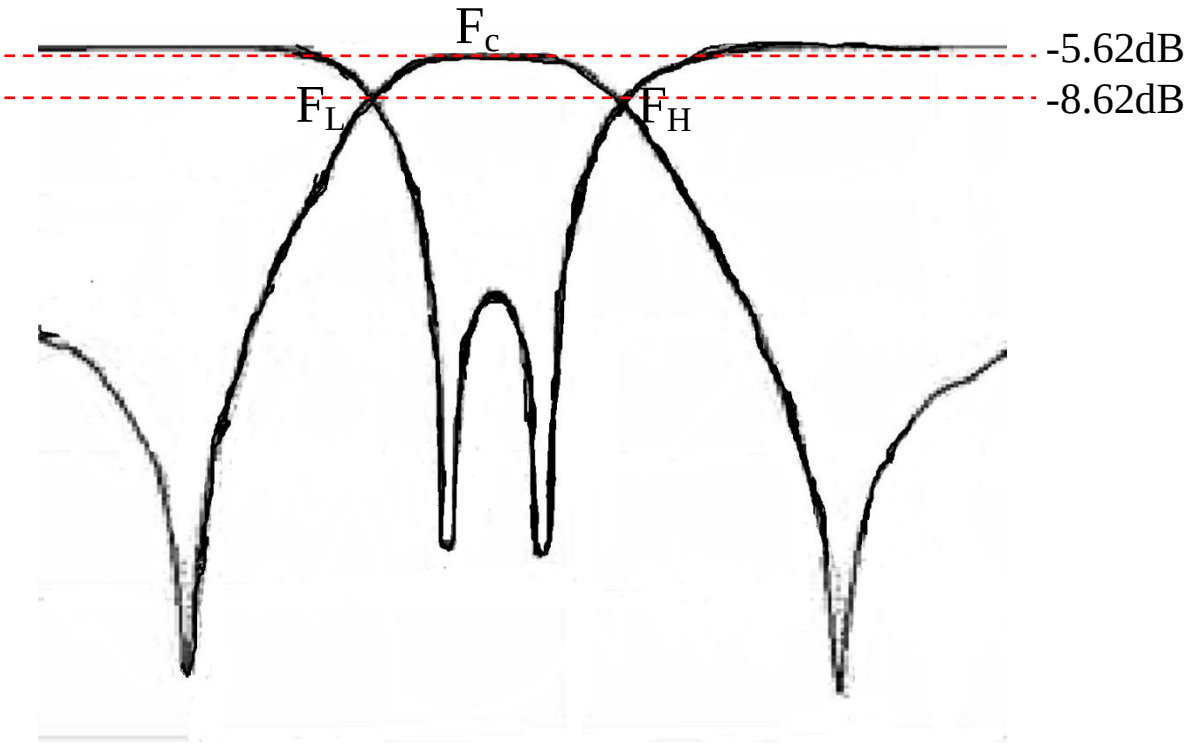

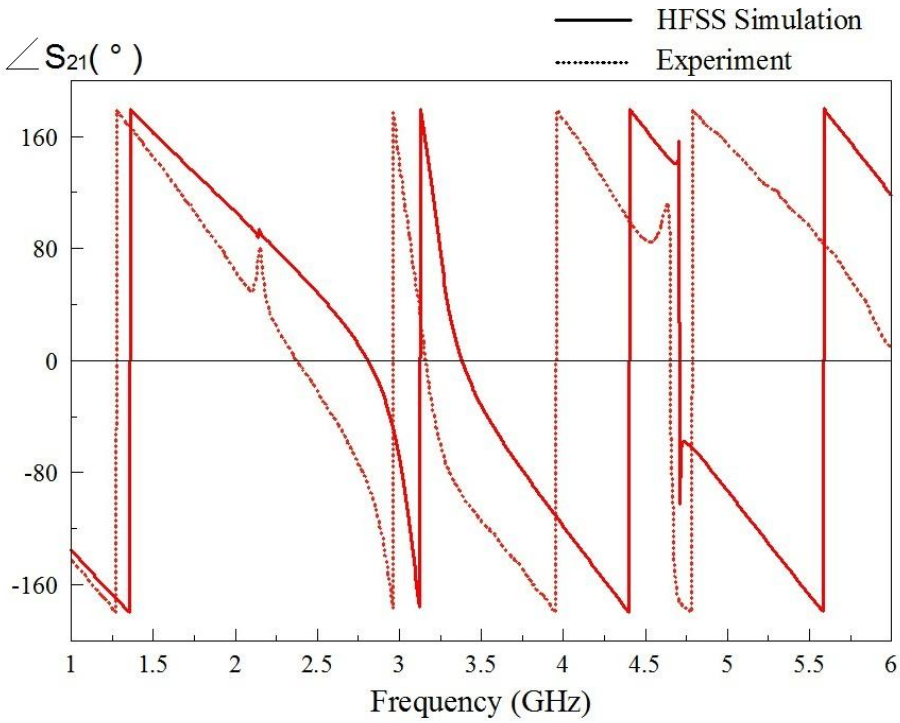

Figure 4.3: Phase angle of simulated and measure S_{21} parameter

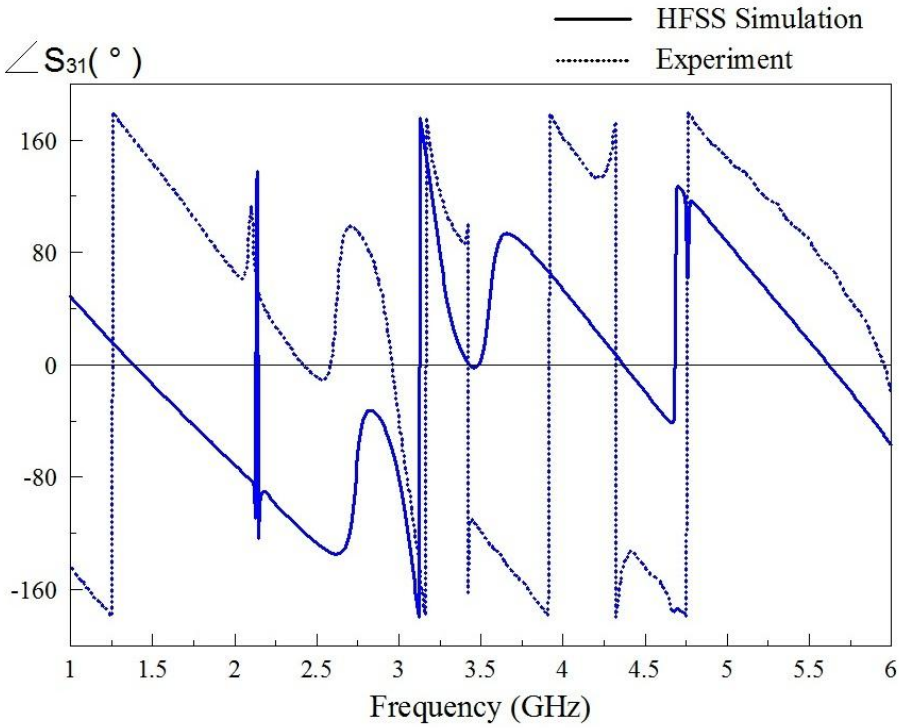

Figure 4.4: Phase angle of simulated and measured S_{31} parameter

4.2 Case Studies

Case study is carried out to study the behaviour and the effect of each parameter to the filter. The parameter that will be studying in this chapter is the cross-slot length, cross-lots width, gap and the inclination angle of the cross-slot. In order to carry out the case studies, only one parameter is change at a time and the rest of the parameters are remained the same. Analysis on the case shows that all the parameters are been optimized. For better comparison, the frequency is made a constant variable.

4.2.1 Cross-slot Length

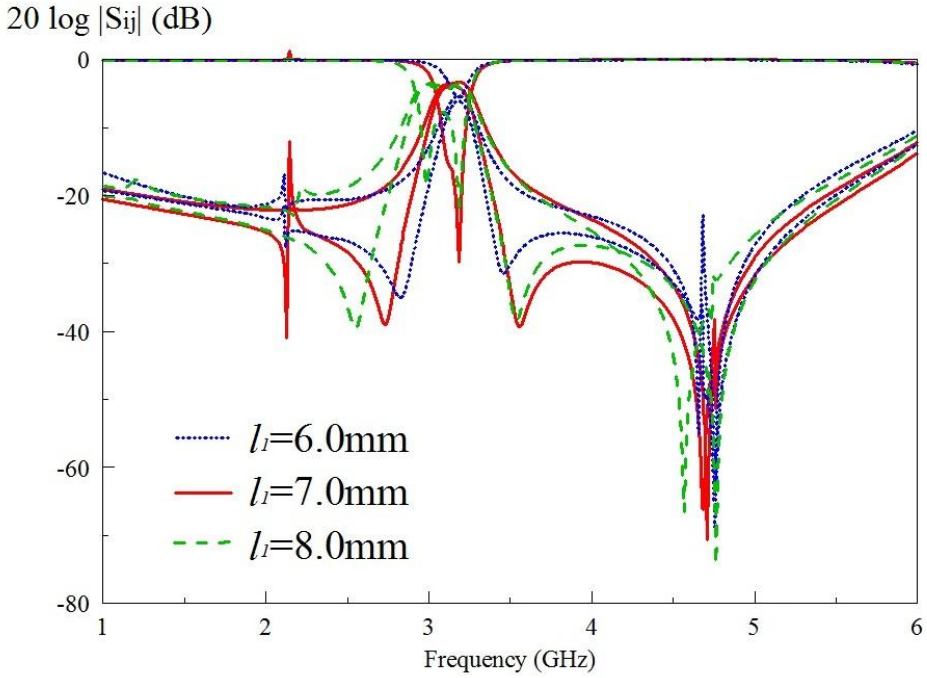

Figure 4.5: Effect of length of the cross-slot, l_1

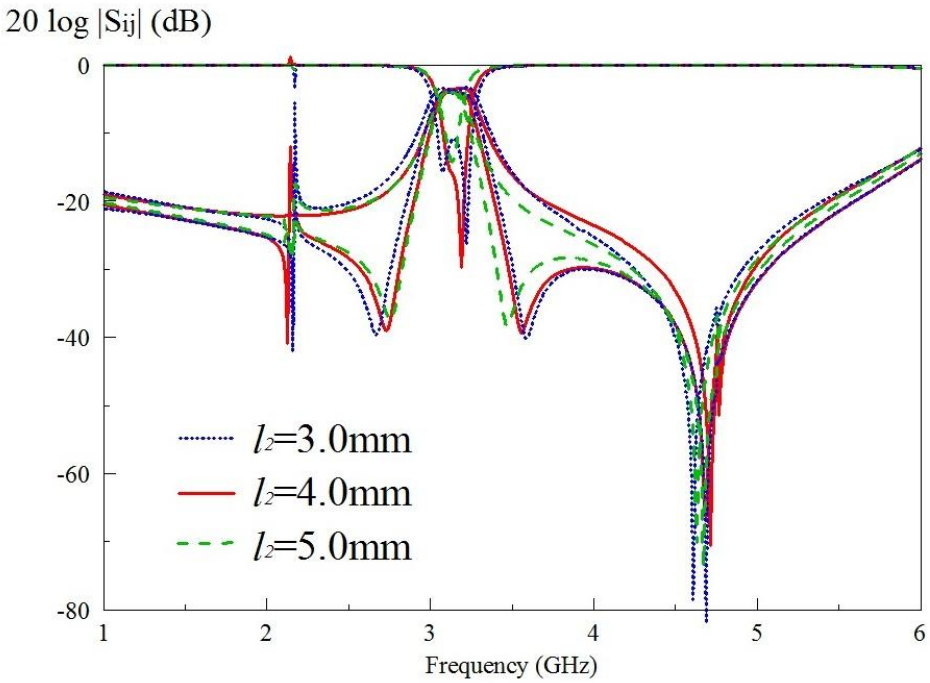

Figure 4.6: Effect of length of the cross-slot, l_2

From Figure 4.5, when the length of the crossed slot l_1 is reduced to 6.0mm, the matching S_{11} deteriorates. The passband becomes narrower and the insertion loss

is reduced from -3dB to -6dB. When the length is increased to 8.0mm, the return loss is more than – 10dB. Both of the modes do not combine well in the passband. Even though the dual-mode characteristic can be seen clearly, it does not produce good results. From Figure 4.6, when the length l_2 is reduced to 3.0mm, an additional mode is generated near to the 2GHz frequency. Both of the modes do not combine well in the passband. When it is 5.00mm the two modes merged well and cannot be seen from the figure.

4.2.2 Cross-slots Width

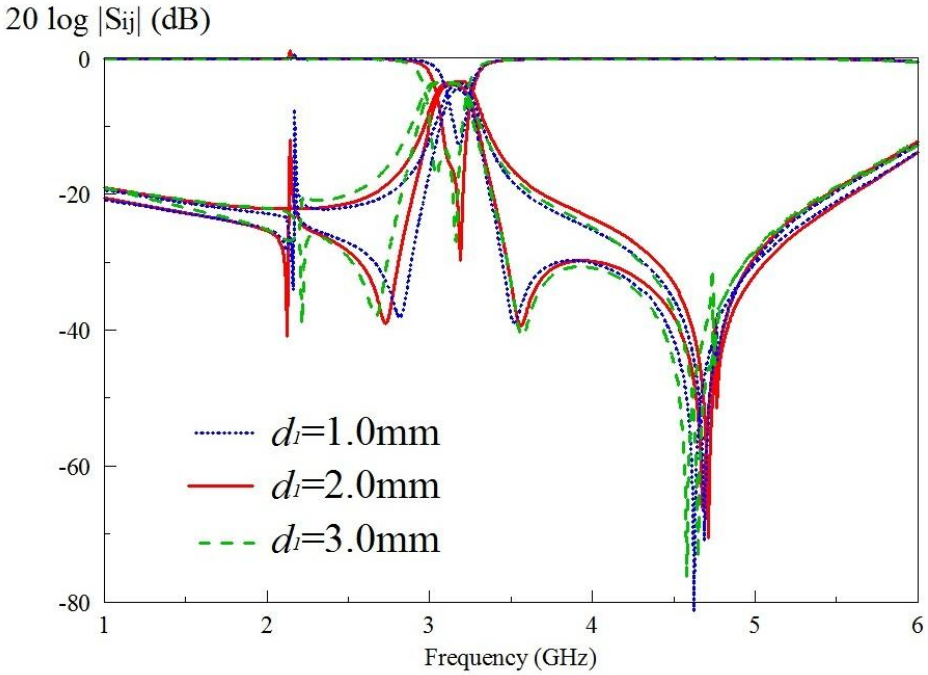

Figure 4.7: Effect of width of the cross-slot, d_1

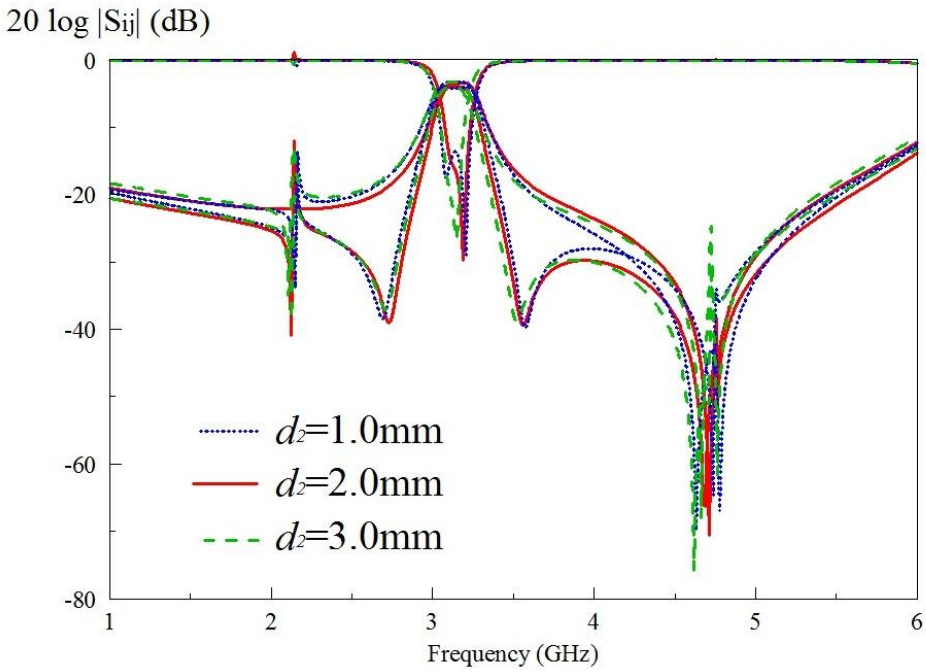

Figure 4.8: Effect of width of the cross-slot, d_2

It can be observed from Figure 4.7, when the width d_1 is reduced to 1.0mm, the insertion loss is increase and the two modes combined. When the width is increased to 3.0mm the two modes do not combine well in the passband. Meanwhile, in Figure 4.8, when the width d_2 is decreased to 1.0mm, there is a big difference between the magnitude passbands of S_{21} and S_{31}. The two modes do not combine well in the passband of S_{21}. When the width d_2 is increased to 3.0mm, only a single mode is seen instead of two modes. There is a big difference between the magnitude passbands of S_{21} and S_{31}

4.2.3 Gap

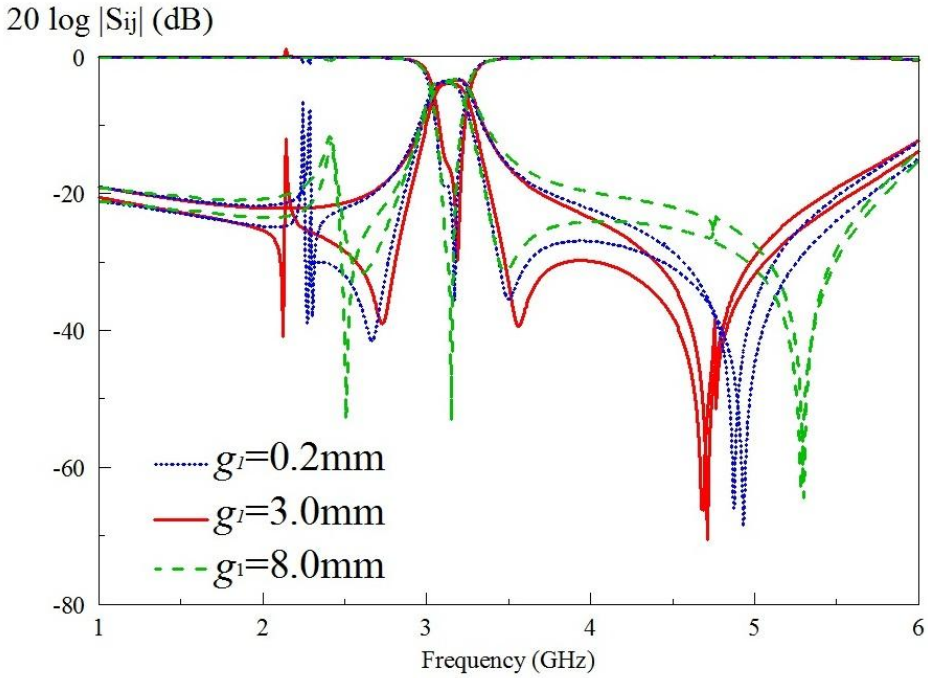

Figure 4.9: Effect of the gap between two coupled lines, g_1

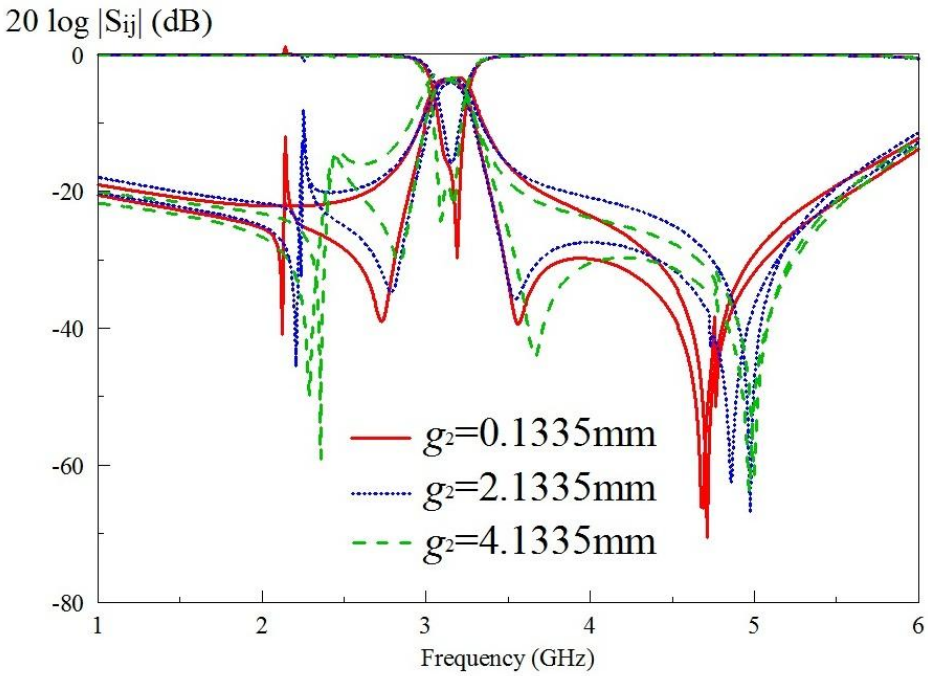

Figure 4.10: Effect of the gap between feedline of port 1 and the edge of coupled lines of port 2 and port 3, g_2

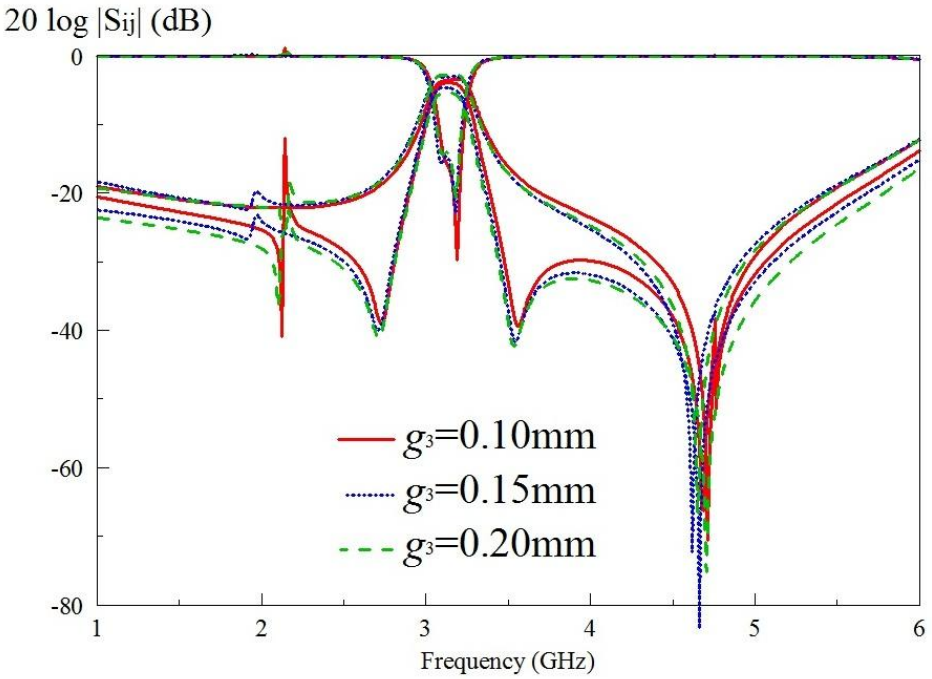

Figure 4.11: Effect of the coupled line with the rectangular patch, g_3

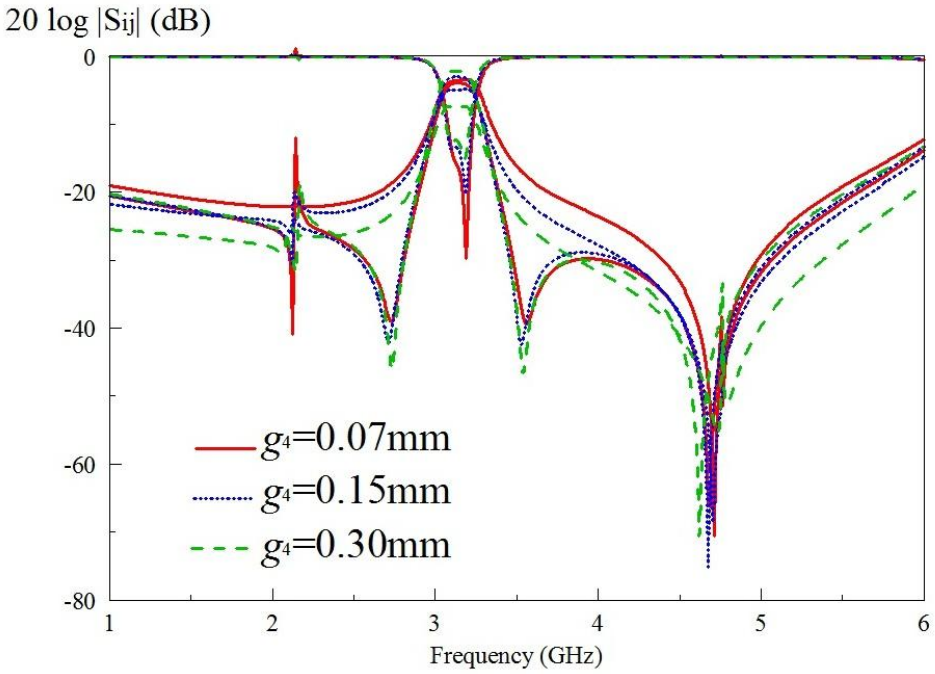

Figure 4.12: Effect of the coupled line with the rectangular patch, g_4

Figure 4.9 to Figure 4.12 show the parametric analysis of the gaps. In Figure 4.9, when the coupling gap between two coupled lines increased to 3.0mm, it does affect the frequency responses significantly and another resonant mode is generated. When the gap further increased to 8.0mm, another resonant mode is generated as

well and only a single mode is seen instead of two modes because both of them combined. From Figure 4.10, when the gap is increased to 2.1335mm, another resonant mode is generated and only a single mode is seen instead of two modes because the two modes combined. When the gap is increased to 4.1335, the insertion loss of both S parameters frequency range is changed and another resonant mode is generated. Figure 4.11 is to analyse the coupling gap between the feedline of port 3 to the rectangular patch. The increase in coupling gap will increase the difference between the magnitude passbands of S_{21} and S_{31}. The differences between the magnitude passbands of S_{21} and S_{31} are -1.5dB and _2.6dB for 0.15mm and 0.20mm respectively. Figure 4.12 shows the analysis of coupling gap between the feedline of port 2 to the rectangular patch. The increased of the coupling gap will also increased the difference between the passband of S_{21} and S_{31}. Hence, the differences between the magnitude passbands of S_{21} and S_{31} are -1.9dB and -5.3dB for 0.15mm and 0.30mm respectively.

4.2.4 Inclination Angle

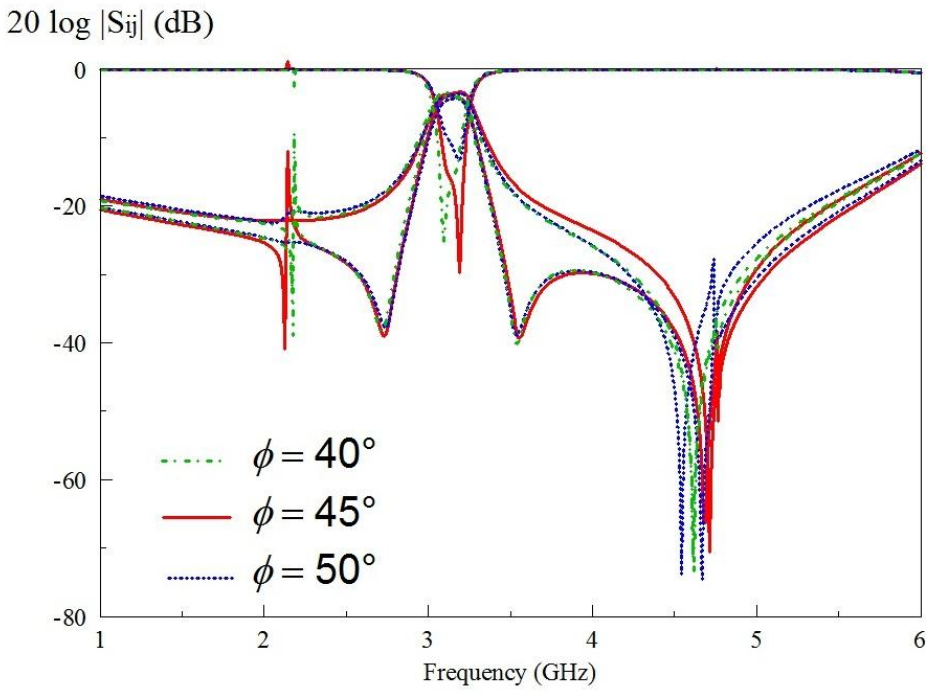

Figure 4.13: Effect of inclination angle, ϕ' on S parameters

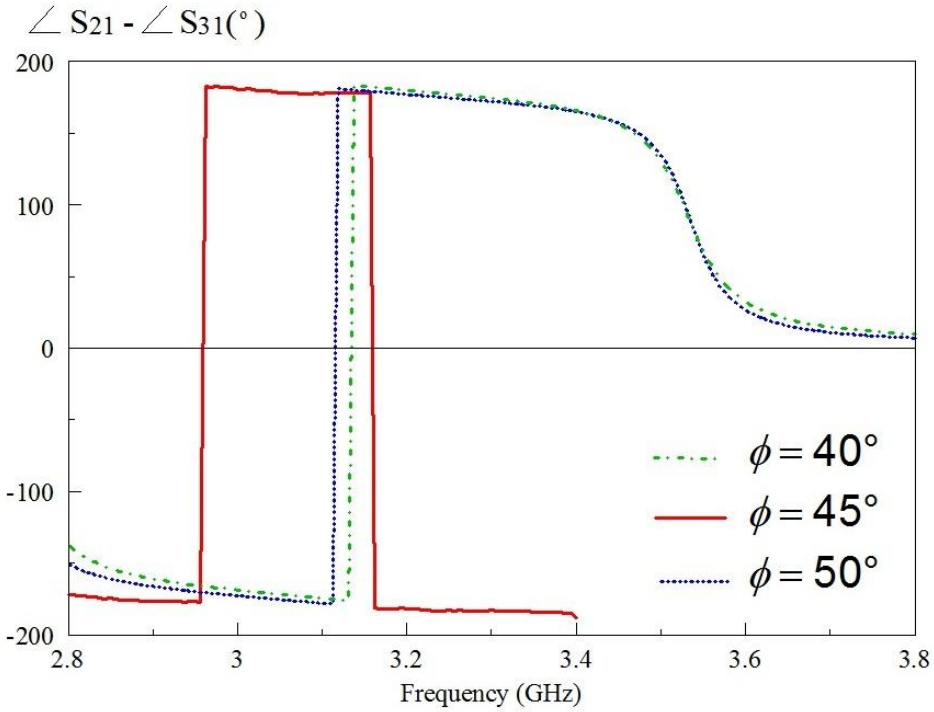

Figure 4.14: Phase different between S_{12} and S_{13} parameter at different inclination angle

In Figure 4.13, only a single mode is seen instead of two modes when the inclination angle is reduced to 40º. There is no significant effect as the inclination angle increased to 50º. It only affects the phase bandwidth. From Figure 4.14, it can be observed that the phase bandwidth is seriously affected.

CHAPTER 5

CONCLUSION AND RECOMMENDATIONS

5.1 Conclusion

In this project, the idea of microstrip patch balun bandpass filter has been proposed. A microstrip patch balun bandpass filter has been demonstrated by using an unequal cross-slot etched on a microstrip rectangular patch. The cross-slot is used to generate two degenerate modes and it works as two independent dual-mode filter in the signal paths of Port 1 - 2 and Port 1 - 3. At the same time, it is a good balun that divides a microwave signal evenly into two with 180^0 out of phase.

Experiments had been carried out and a reasonable and good agreement had been observed between the simulated and measured results. The filter has been successfully fabricated on a RT/Duroid 6006 substrate. In addition, the author had acquired the knowledge and skill of doing research and carry out experiments independently. The understanding of microwave engineering theory and concept had greatly improved after completing this project. In conclusion, the aim and objectives of this project had been achieved.

5.2 Recommendation

The proposed microstrip patch balun filter can be further improved where the capacitive coupled feed lines gap can be further decrease. However this is unable to be done in the laboratory due to lack of technology on fabricating the filter. Only high technology which uses laser light to etch the microstrip line will able to produce a fine narrow line up to 0.02mm. Narrower coupled feed lines can increase the insertion lost to exactly –3dB. Moreover, a multilayer approach can be incorporated into the proposed patch balun filter to produce a multilayer balun filter. This approach is difficult to design as it needs a high dielectric constant substrate for both layers so that the signal can be go through from bottom layer to the top layer. RT/Duroid 6010 substrate has high dielectric constant but it is expensive and will produce high radiation loss. Hence, further research need to be done on this area to make this idea successful in the future.

The proposed balun filter/power divider only can divide one microwave signal equally into two. Hence, in future more output can be design on the filter where one microwave signal can be divided into several output equally with same magnitude. This will be a new research area for microwave filter. In conclusion, there are still many areas on microwave engineering that need further research into to produce more filter with good features and contribute to wireless communication development.

REFERENCES

Band Pass Filter. (n.d.) Wikipedia. Retrieved March, 2011 from http://en.wikipedia.org/wiki/Band_pass_filter

Microstrip-Microwave Encyclopedia. (20,August 2010). Retrieved March 2011, from microwaves101.com: http://www.microwaves101.com/encyclopedia/microstrip.cfm

Zhu Lei, Pierre-Marie Wecowski, and Ke Wu, "New Planar Dual-Mode Filter Using Cross-Slotted Patch Resonator for Simultaneous Size and Loss Reduction", IEEE Microwave Theory and Techniques, vol. 47, pp 650-654, 1999

Y. Sung, "Compact and Low Insertion Loss Dual-Mode Bandpass Filter", Microwave and Optical Technology Letters, vol. 50, No. 12, pp 3201-3206, December 2008

Kittisak Phaebua and Chuwong Phongcharoenpanich, "Characteristics of a Microstrip Semi-Circular Patch Resonator Filter", ECTI-CON 2008. 5th Internation Conference, vol. 1, pp 273-276, 2008

J. K. Xiao, Q. X. Chu and S. Zhang, "Novel Microstrip Triangular Resonator Bandpass Filter with Transmission Zeros and Wide Bands Using Fractal-Shaped Defection", Progress In Electromagnetics Research, vol. 77, pp 343-356, 2007

X. Wang, J. Zou and Y. Li, "New Compact Microstrip-Patch Bandpass Filter with Two Transmission Zeros", Microwave and Optical Technology Letters, vol. 42, pp 315-317, 20 August 2004